Investigation of G1 Arrest Mechanisms Induced by *Sanguisorba officinalis* Extracts in B16F10 Cells

Tan, Yi-Hsun

Table of Contents

List of Figures

List of Table

Summary of Abbreviations

AKT	protein kinase B
CK2	Casein kinase 2
CP	cisplatin
DMSO	Dimethyl sulfoxide
EA	ellagic acid
FACS	fluorescence-activated cell sorting
FAK	focal adhesion kinase
FBS	fetal bovine serum
FT-IR	Fourier transform infrared spectroscopy
MAPK	Mitogen-activated Protein Kinase
PIP2	phosphatidylinositol 4,5-bisphosphate
PIP3	phosphatidylinositol (3,4,5)-trisphosphate
PI3K	phosphoinositide 3-kinase
PTEN	Phosphatase and Tensin Homolog Deleted from Chromosome 10
p70S6K	ribosomal protein S6 kinase beta-1
SPE	solid phase extraction

Abstract

Losing controls on cell cycle, cell growth, and cell death usually lead to cancer development, which threatening many people's lives all over the world. The poor prognosis of advanced cancer underscores the urgency of continuing efforts to find new effective strategies. In Chinese medicine, herbal medicine is commonly used to treat individuals suffering from many types of diseases. I thus expected that some herbal medicines would contain promising compounds for cancer therapy. Indeed, *Sanguisorba officinalis* extracts were observed to effectively inhibit the growth of B16F10 melanoma cells. I proposed a simplified method to purify the responsible ingredient, which was then identified as ellagic acid (EA). B16F10 cells treated with EA exhibited strong G1 arrest accompanied by accumulation of p53, followed by attenuation of the AKT signaling pathway. Addition of a PTEN inhibitor, but not a p53 inhibitor, abrogated all the EA-induced phenotypes including AKT inactivation and G1 arrest. The PTEN inhibitor also diminished EA-induced p53 accumulation. Furthermore, EA apparently increased the protein phosphatase activity of PTEN, as demonstrated by the reduced phosphorylation level of FAK, a protein substrate of PTEN. Moreover, an *in vitro* PTEN phosphatase assay on PIP3 showed the direct modulation of PTEN activity by EA. These results collectively suggest that EA functions as an allosteric modulator of PTEN, enhancing its protein phosphatase activity while inhibiting its lipid phosphatase activity. Last, I proposed a therapeutic strategy using a combination of EA and cisplatin, a broadly used chemotherapy agent. The combination dramatically enhanced cell death and inhibit cell proliferation for extended periods in B16F10 cells, suggesting a promising possibility in chemotherapy application.

1. Introduction

1-1 Cell cycle control and cancer development

Cancer development arises from and progresses via the accumulation of abnormal alterations in genes related to cell growth, cell cycle control, and cell death [1,2], which eventually leads to uncontrolled proliferation of the cells. The cell cycle normally arrests at defined checkpoints: the G1 checkpoint, the G2/M checkpoint, or the metaphase checkpoint, if the appropriate signals for the progression are not elicited [3,4] (fig. 1). The ability of cells to undergo cell cycle arrest is a crucial factor for maintaining genomic stability, and the dysregulation of the cell cycle usually leads to cancer development [3,4]. Regulation of the cell cycle relies on the activities of cyclin-dependent kinases (CDKs) [4-6], which are dependent on the quantities of cyclins and the binding of the inhibitory proteins [4,6,7]. The activated cyclin-CDK complexes then in turn, activate downstream targets to promote or prevent cell cycle progression. The expression of cyclins and the inactivation of their inhibitory proteins are under exacting control to ensure that cells appropriately progress through the cell cycle [4-7]. Cancer cells tend to lose some of the aforementioned controls; for instance, continuously activated proliferative kinases, such as MAPK or PI3K/AKT [8-10], facilitate abnormal cell cycle progression and survival. Loss-of-function mutation or loss of heterozygosity of tumor suppressor genes, such as PTEN or p53, is commonly found in cancer cells and results in abnormal proliferation [11-14]. Terminating the uncontrolled cell cycle progression is an attractive strategy for cancer therapy, and therefore, is of great interest in translational research.

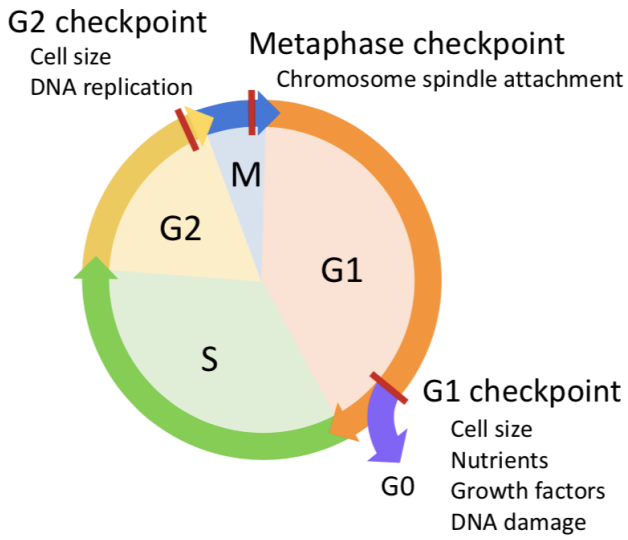

Fig. 1 The cell cycle checkpoints

1-2 G1 checkpoint

The G1 checkpoint, also known as the restriction point in mammalian cells, is the point that the cell is committed to entering the cell cycle. To get through G1 checkpoint (Fig. 2), stimulation of mitogen signaling pathways, such as Ras-Raf-MEK-ERK or PI3K-AKT-mTOR, are required[15,16]. Activation of these pathways increases the expression and stability of cyclin D[15], which binds to and activates CDK4 or 6[17]. AKT also phosphorylates the CDK inhibitory proteins, such as p21 and p27, preventing their nuclear import and decreasing their stability[18,19]. Moreover, AKT promote Mdm2-mediated ubiquitination and degradation of p53[20], the transcription factor targeting p21 expression. The E2F transcription factors, which target many genes with activating ability, is bound to and restrained by its inhibitory protein pRb[21,22]. Activated CDK4/6-cyclin D complex phosphorylates pRb, releasing E2F and in turn, push forward the cell cycle progression[21,22].

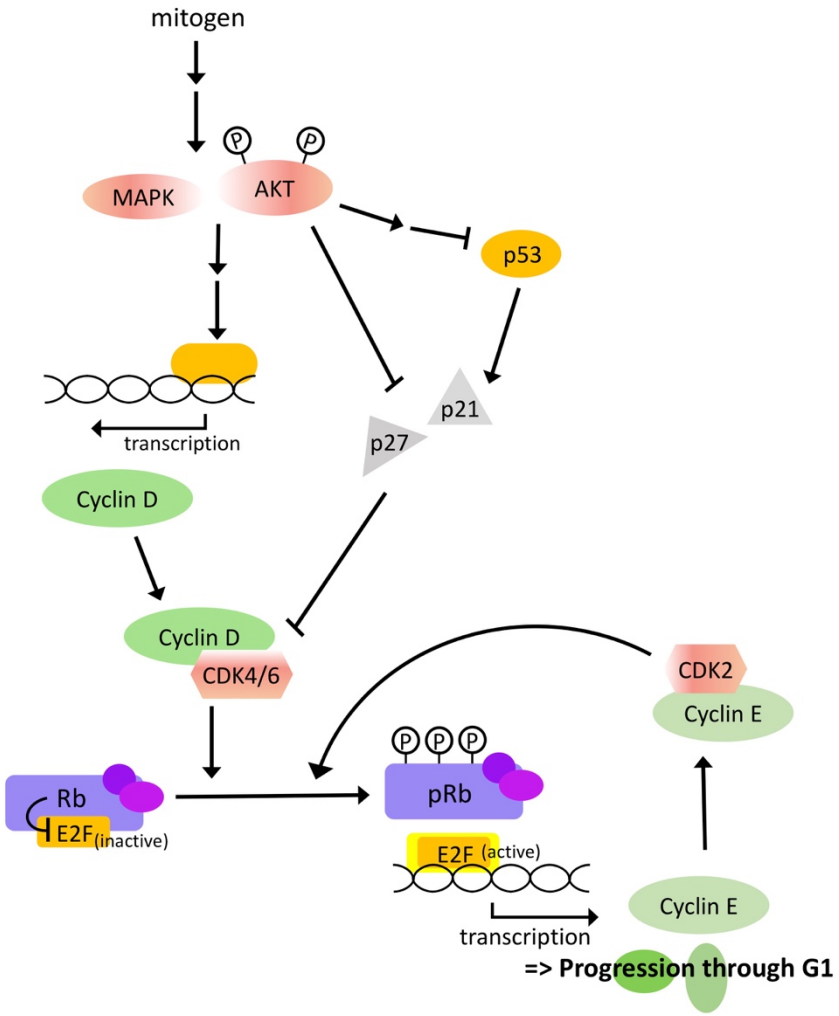

Fig. 2 The key proteins involved in the progression through the G1 restriction point

1-3 The PI3K-AKT Cell growth promoting signaling pathways

The PI3K-AKT signaling is important for the regulation of multiple biological processes [23]. Extracellular stimulating signals activates PI3K, which phosphorylates and turns PIP2 into PIP3[24] (Fig. 3). Accumulation of PIP3 recruits cytosolic inactive AKT to the membrane where it is activated by PDK1 and mTORC2, which are also dependent on PIP3[25]. Signal termination could be achieved by PTEN, a dual lipid/protein phosphatase with the opposite activity to PI3K[23,24]. Activated AKT then phosphorylates its downstream effectors, such as GSK3, mTORC1, and FOXO1, which play critical roles in metabolism, cell growth, cell cycle progression, and apoptosis[24,26]. Amplification or oncogenic somatic mutations in growth factor receptors, PDK1, or PI3K results in hyperactivation of AKT, which is usually observed in human cancers[8,23]. Similarly, loss-of-function mutations in PTEN or AKT phosphatase also lead to abnormal AKT activation. PI3K/AKT inhibition are often applied for cancer treatments with hyperactivated AKT[27-29]. However, feedback activation of AKT during treatments of patients with PI3K inhibitors is a problem in cancer therapy as well as biological experiments[29]. Therefore, it is important to find novel strategy that effectively governing the uncontrolled AKT activation.

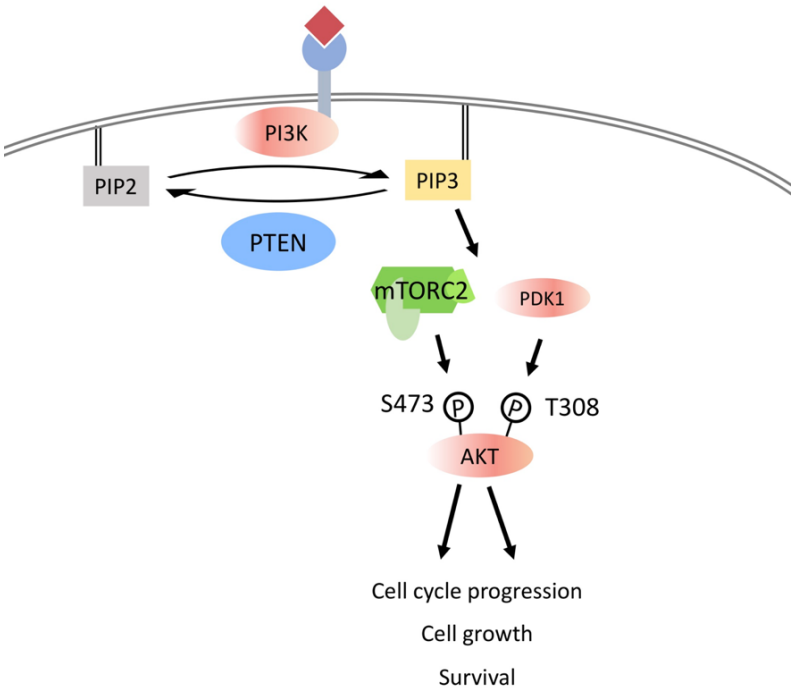

Fig. 3 The PI3K-AKT pathways

1-4 Melanoma

Malignant melanoma is one of the most invasive types of cancer [30,31]. Unresectable advanced melanoma is quite resistant to chemotherapy, which translates to an extremely poor survival rate [31-33]. Most of the current treatments show low response rates and manifest little effect on survival of the melanoma patients[34]. Furthermore, the incidence of melanoma is keeping rising on a global level [30,35]. Recently, novel antibody-based drugs have been developed, and these have produced dramatic remissions in certain patients with advanced stages of malignant carcinoma[36,37]. However, the drugs are really expensive, and the efficacies are limited to approximately 30% of melanoma patients, at best[37]. These facts underscore the urgency of continuing efforts to find new effective strategies for malignant melanoma therapy.

1-5 The plant extract and the aim of this study

A few years ago, in our lab, a plant extract was found to manifest anti-Alzheimer's Disease activity[38]. Encouraged by this discovery, I speculated that some plant extracts used in Chinese herbal medicine might harbor preferential anti-cancer activities. After screening kinds of plant extracts, an ethanol extract of the dried root of Garden Burnet (*Sanguisorba officinalis*) was found to manifest anti-proliferative effects accompanied by G1 arrest on B16F10 malignant melanoma cells. *Sanguisorba officinalis* is an herbaceous plant distributed throughout the cooler regions in Europe, Asia, and North America. It has been used as a traditional Chinese medicine for treatment of hematemesis, melena, intestinal infections, and inflammatory diseases for decades [39-41] . Recently, its extract was found to induce cell cycle arrest and cell death in gastric carcinoma and breast cancer cell lines [42,43]. However, its effects on melanoma cells and the mechanism of how it induces cell cycle arrest are not yet well understood.

In this study, first, I purified and identified the compound responsible for inducing cell cycle arrest. Next, I further characterized and provided novel insights as to how the compound induces cell cycle arrest, suggesting new leads for therapeutic intervention. And last, I proposed a novel combination therapeutic strategy using the purified chemical.

2. Materials and Methods

2-1 Materials and Reagents

Materials, reagents, and vendors are as follows:

- Cell culture: Roswell Park Memorial Institute medium 1640 (RPMI 1640); phosphate buffer saline (-) (PBS) (NACALAI TESQUE); fetal bovine serum (FBS) (Sigma, St. Louis, MO, USA); 10cm dishes (FPI, Japan); 24-well plates (Thermo Fisher Scientific).
- Purification process: Oasis MAX column (Waters); Mightysil RP-18 GP150-4.6 (5 μM) column (KANTO Chemical).
- FACS analysis: RNaseA (Roche); propidium iodide (PI) (NACALAI TESQUE); BD FACS Calibur (BD Biosciences).
- Western Blot: EDTA free protease inhibitor cocktail (NACALAI TESQUE); Protein Assay Bicinchoninate Kit (Nacalai Tesque); PVDF membrane (Pall corporation)
- Cell death: trypan blue stain (Thermo Fisher Scientific).
- Chemical treatments: Ellagic acid (LKT Laboratories); VO-OHpic trihydrate (Abcam); Pifithrin-α-HBr (Abcam); LY294002 (Abcam); Cisplatin (Nippon Kayaku).
- *In Vitro* phosphatase assay: Malachite Green Phosphatase Assay Kit (Echelon K-1500); phosphatidylinositol 3,4,5-trisphosphate diC8 (PI (3,4,5) P3 diC8) (Echelon Biosciences); Recombinant PTEN enzyme (Echelon Biosciences).

2-2 Cell culture

The B16F10 (obtained from Riken Bioresource Center Cell Bank) mouse melanoma cell line was cultured in RPMI 1640, with 10% FBS in 5% CO_2, in a 37°C humidified incubator.

2-3 Plant crude extract

An ethanol extract of *Sanguisorba officinalis* was purchased from an import company of Chinese medicine.

2-4 Bligh-Dyer method

Crude plant extract was dissolved in a solvent mixture in the ratio of 1 g crude: 10 ml chloroform: 20 ml methanol: 8 ml H_2O, and mixed thoroughly by vortexing and incubating at room temperature (RT) for over 20 min. Then, 10 ml ddH_2O and 10 ml chloroform were added followed by incubation for over 30 min at RT. The sample was then vortexed and centrifuged (10,000 *g*, 15 min) to separate the organic-soluble (F1) and water-soluble (F2) fractions.

2-5 Solid-Phase Extraction

An Oasis MAX column was used for separation. Dried F1 / F2 fraction was dissolved in basic buffer (1.0% $(C_2H_5)_3N$ in 0.2% $CH_3COOH_{(aq)}$) and slowly passed through the column. After washing the column with the same buffer, the samples were eluted with Methanol, and the neutral compounds (F1-N fraction) was collected. Lastly, the column was eluted with 2% $HCOOH_{(MeOH)}$, and the basic compounds (F1-B fraction in figure 6c, 6d) was collected.

2-6 Decantation

5 ml acetonitrile was added to a 15 ml centrifuge tube with 80 mg sample. Water bath sonication was performed to resuspend the insoluble compounds thoroughly before centrifugation (10,000 *g*, 3 min.). The supernatant was discarded and the previous steps were repeated for at least 5 times before drying the samples using a vacuum dryer.

2-7 Pyridine recrystallization

60 mg sample was fully dissolved in 4 ml pyridine after heating the solution to around 80 °C in a water bath. The sample was placed on ice, and after recrystallization, the crystal was recovered by vacuum filtration.

2-8 HPLC analysis

A Mightysil RP-18 GP150-4.6 (particle size 5 μM) column was used for separation. The mobile phase of HPLC analysis was 0.1% formic acid, 40% acetonitrile in H_2O (isocratic elution), with a flow rate of 1 ml/min. Samples were dissolved in the same solution. HPLC chromatograms were acquired at 254 nm and recorded on an Alliance 2690 HT (Waters, Massachusetts, USA), 996 Photodiode Array Detector (Waters).

For the quantification of EA in the crude extract, EA solution was made in concentration of 2, 10, 20, 50 μg/ml, and the height of peaks were calculated to make standard calibration curve. S*anguisorba officinalis* extract was dissolved in the HPLC solution in concentration between 700-2,000 μg/ml.

2-9 NMR analysis

^{1}H-NMR spectra were recorded on a JNM-AL 400 (JEOL, Tokyo, Japan) at 400MHz. Chemical shifts were reported relative to residual solvent of DMSO- d_6 (δ 2.49). Multiplicity was indicated by one or more of the following: s (singlet); bs (broad singlet). ^{13}C-NMR spectra were recorded on a JNM-AL400 (JEOL) at 101MHz. Chemical shifts were reported relative to residual solvent of DMSO- d_6 (δ 39.5).

2-10 FT-IR analysis

The IR spectra were obtained by an FT/IR-4100 Fourier-transform infrared spectrometer with attenuated total reflectance (JASCO, Japan).

2-11 Mass Spectrometry

High-resolution mass spectra were recorded on an LCMS-IT-TOF (Shimadzu) for electrospray ionization (ESI)-MS.

2-12 Melting point measurement

Melting point (mp) was determined on BUCHI Melting Point M-565 (BUCHI, Postfach, Switzerland) micro melting point apparatus.

2-13 Chemical treatments

Ellagic acid, Pifithrin-α-HBr, VO-OHpic trihydrate, LY294002, plant crude extract, and the intermediate compounds collected throughout the extraction process from crude plant to ellagic acid were dissolved in DMSO. Cisplatin was dissolved in ddH_2O. All treatment conditions received DMSO at a final concentration of 0.5%.

2-14 Cell cycle analysis

After various treatments, cells were lightly washed with PBS and harvested using 0.25% trypsin -EDTA. Culture medium, wash liquid (PBS), and cells were all collected into 15 ml centrifuge tubes and centrifuged (800 *g*, 5 min, room temperature) to harvest all the cells including the dead ones. The cells were resuspended in 0.3 ml PBS and transferred into 1.5 ml tube before being fixed in 70% ethanol at 4°C for over 4 hours. Before FACS analysis, cells were treated with 500 μg/ml RNaseA for 30 min at room temperature, followed by staining with 50 μg/ml propidium iodide (PI) on ice. 10,000 cells were counted for analysis by BD FACS Calibur. The data were analyzed using BD Cell Ques+ Pro (Version 5.2). FL2A was selected as the vertical axis of the histogram chart to display the relative DNA content.

2-15 Cell Proliferation assay of ellagic acid and cisplatin combined treatment

3 x 10^4 cells were plated per well in 24-well plates. After 24-hour incubation, cells were treated with 0, 5, 10 μg/ml EA combined with 0, 15, 30 μM cisplatin for 24 hours (day 1), then the treatments were halted by replacing the medium with fresh medium lacking EA and cisplatin. The living cell numbers were counted by Trypan blue assay on day 1, 2 (1 day after removal of EA and cisplatin), 3, 5 and day 7, or until the cell proliferation exceeded 10 times the cell density determined on day 0.

2-16 Trypan Blue analysis

After various treatments, cells were washed with PBS and harvested using 0.25% trypsin - EDTA. Cells, culture medium, wash liquid (PBS) were all collected into 1.5 ml tubes and centrifuged (800 *g*, 5 min, room temperature) to harvest all the cells including the dead ones. The pellets were resuspended in 100 μL PBS. 10 μL of the PBS suspension were mixed thoroughly with 10 μL 0.4% trypan blue stain in and the living cell numbers and ratios were counted using countess II FL.

2-17 Western blot analysis

Cells in 60 mm dishes were washed with 1 ml PBS and the attached ones were collected by adding 120-200 μL RIPA buffer and scraping, with the volume of RIPA buffer depending on the cell density. Brief sonication to lyse cells was followed by centrifugation at 15.000 *g*, 4°C for 3 min and collection of supernatants. The protein concentration was estimated by a Protein Assay Bicinchoninate kit and diluted to a concentration of 7-10 μg/uL with RIPA buffer and SDS protein loading dye.

7 μg of total protein was loaded per lane, and proteins were separated by 12% SDS-PAGE and transferred to a PVDF membrane. The blots were blocked in 5% BSA TBS-T buffer for 1-2 hours at room temperature and were then incubated with the primary antibody at 4°C

overnight, followed by 50 min secondary antibody binding at room temperature. Amersham™ ECL™ Western Blot Detection Reagent was used for signal detection.

RIPA buffer: 0.5 mM DTT, 1 mM EDTA, 0.1% CHAPS, 5 mM β-glycerophosphate, 1 mM NaF, 1 mM $NaVO_4$, 1 mM NaPPi, 0.5 mM PMSF, EDTA free protease inhibitor cocktail (1:100).

The primary antibodies used for Western blot are listed in table 1. Secondary antibodies labeled with HRP were purchased from GE Healthcare, and signals were visualized by enhanced chemiluminescence (GE Healthcare). Signal intensities for the statistical data were calculated using ImageJ, and the protein amount was normalized to actin, the loading control.

Table 1. List of antibodies.

Antibody	vendor	Catalog number	Dilution
Anti-actin	Millipore	MAB1501	1: 2,500
Anti-p53 (FL-393)	Santa Cruz Biotechnology	sc-6243	1:200
Anti-p21 (C-19)	Santa Cruz Biotechnology	sc-397	1:200
Anti-cyclin D1 (H-295)	Santa Cruz Biotechnology	sc-753	1:200
p-AKT (Ser473) (D9E)	Cell Signaling Technology	#4060	1:2,000
anti-phosho-AKT (Thr308)	Cell Signaling Technology	#4056	1:1,000
anti-AKT	Cell Signaling Technology	#4691	1:1,000
anti-phosho-p70S6K (Thr389)	Cell Signaling Technology	#9234	1:1,000
anti-p70S6K	Cell Signaling Technology	#2708	1:1,000
anti-phosho-p44/42 MAPK (Thr202/Tyr204)	Cell Signaling Technology	#9101	1:1,000
anti-p44/42 MAPK	Cell Signaling Technology	#9102	1:1,000
anti-PTEN	Abcam	ab32199	1:5,000
anti-phospho-CK2 substrate [(pS/pT)DXE]	Cell Signaling Technology	#8738	1:1,000
anti-phosho-FAK (Tyr397) (D20B1)	Cell Signaling Technology	#556	1:1,000
anti-FAK	Santa Cruz Biotechnology	sc-271126	1:200

2-18 PTEN Activity Assay

PTEN lipid phosphatase activity was measured by the dephosphorylation of phosphatidylinositol 3,4,5-trisphosphate diC8 (PI (3,4,5) P3 diC8). Recombinant PTEN enzyme was reconstituted in distilled water to yield a concentration of 50 μg/ml just before the start of the assay. EA/VO-OHpic trihydrate dissolved in DMSO was added to the PTEN reaction buffer (25 mM Tris-Cl pH7.4, 140 mM NaCl, 2.7 mM KCl, 10 mM DTE) to achieve the indicated concentration. Each reaction contained 75 ng PTEN enzyme, and 3 nmol of PIP3 was added (final volume of 25 μL) to start the reaction. After the indicated reaction duration in 37°C, 100 μL of Malachite Green Solution was added to terminate the reaction. After 20 min of development of the color at room temperature, the absorbance at 600 nm was measured. The phosphate amount was calculated by interpolating experimental values into the standard curve (phosphate standard: Echelon K-1500 kit).

2-19 Statistical Analysis

The statistical significance was tested by a one-tailed or two-tailed paired Student's t-test depending on the hypothesis. P values < 0.05 were considered to be statistically significant.

3. Results

3-1 A *Sanguisorba officinalis* extract decreases B16F10 cell numbers

I started the investigation by examining the effects of varying concentration of *Sanguisorba officinalis* extract on the growth of B16F10 melanoma cells. The extract brought about a dose-dependent inhibition in cell proliferation after a 24-hour treatment (Fig. 4a, 4b). Treatment of cells with a higher concentration of extract (300 μg/ml) further elicited a prominent subG1 population (Fig. 4c), typically composed of cells undergoing apoptosis.

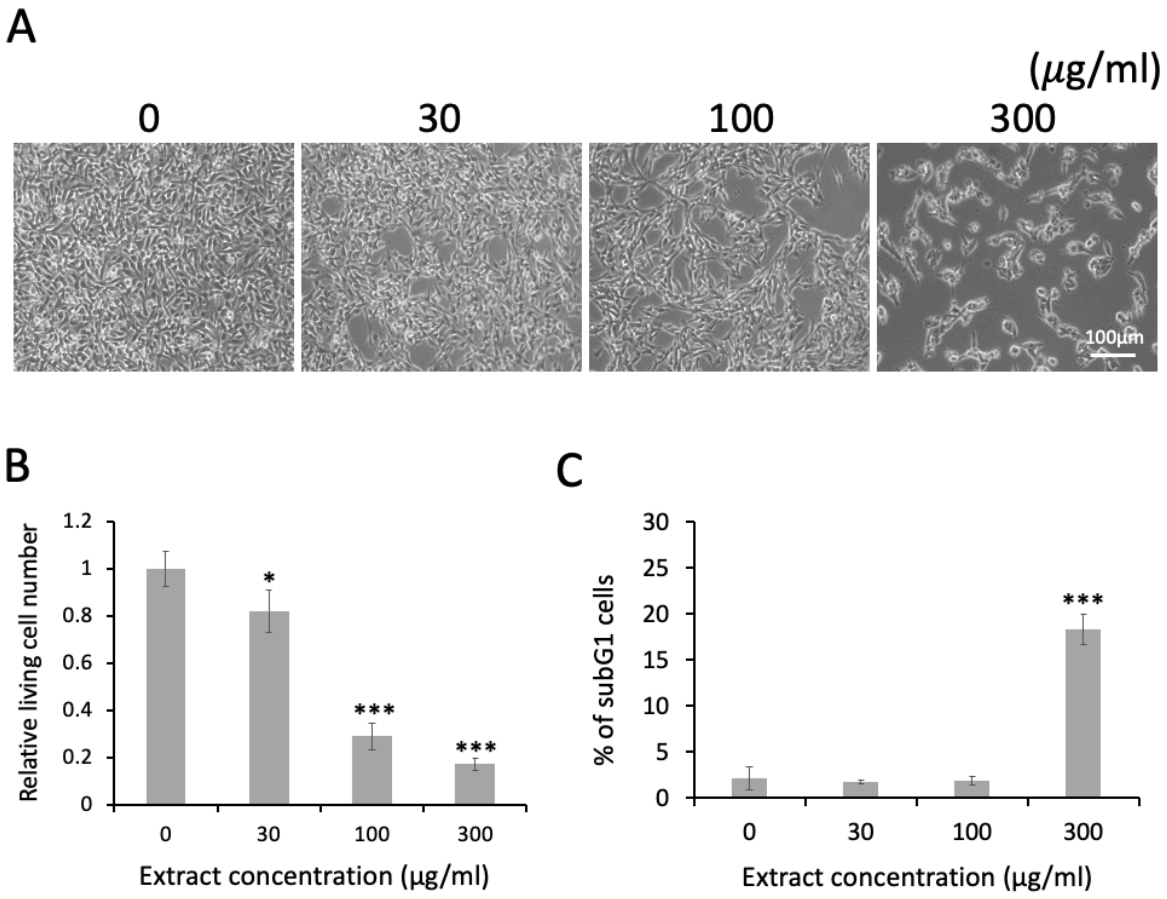

Fig. 4 Extract of *Sanguisorba officinalis* inhibits B16F10 cell growth and inducing cell death

(a, b) B16F10 cells morphology (a) and relative living cell numbers (b) after 24 hr treatments with the labeled concentrations of *Sanguisorba officinalis* extract. Data are means ± SD, student's t-test *: $p < 0.05$, ***: $p < 0.001$.

(c) Percentage of subG1 cells after 24 hr treatments, determined by FACS analysis. Data are means ± SD. ***: $p < 0.001$.

3-2 *Sanguisorba officinalis* extract induced G1 arrest in B16F10 cell

To determine whether the reduction in cell number was related to cell cycle arrest, the distribution of cellular DNA content was measured by FACS. In 0.5% DMSO treated cells (control) (Fig. 5a), about 50% of cells were in G1 phase, whereas approximately 70% of cells treated with 100 μg/ml of *Sanguisorba officinalis* extract were in G1 phase (Fig. 5b, 6a). I assumed that at least one component in the extract harbors the ability inducing G1 arrest, and then performed the following purification experiments.

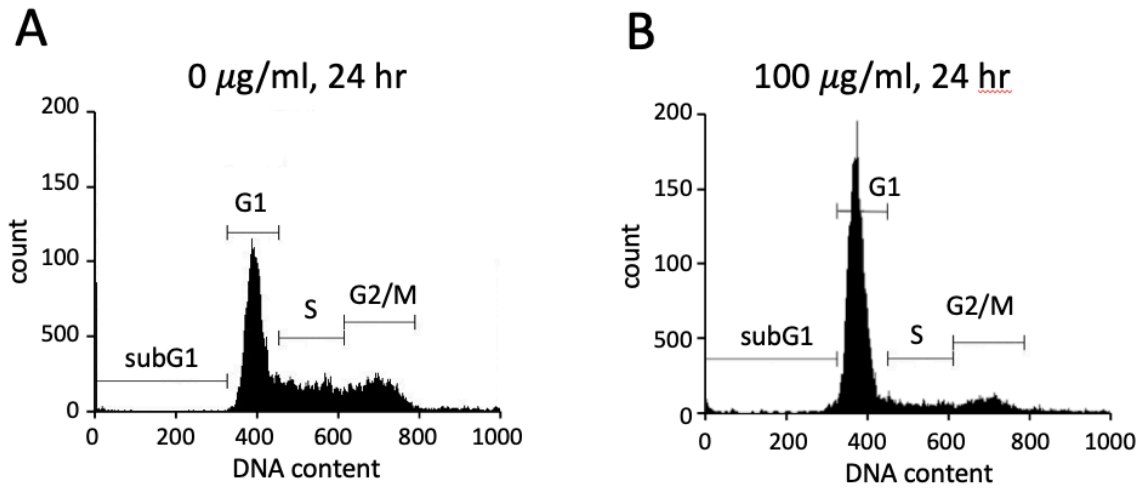

Fig. 5 Extract of *Sanguisorba officinalis* induced G1 arrest in B16F10 cell

(a,b) Cell-cycle profiles based on PI fluorescence intensity after 24 hr DMSO control (a), 100 μg/ml (b), *Sanguisorba officinalis* extract treatment.

3-3 An active compound was purified from the *Sanguisorba officinalis* extract

To purify the active compound responsible for inducing G1 arrest, I first conducted Bligh-Dyer method to separate the organic-soluble and the water-soluble components. The organic fraction in the Bligh-Dyer method appeared to have higher activity in inducing G1 arrest than the aqueous fraction (Fig. 6a). HPLC analysis determined that 3 main components, labeled as A, B, and C in figure 6b, were present in the organic fraction. The chemical released at 2.019 min (component A in Fig. 6b) was deemed to be the responsible compound, since the results of an SPE Oasis MAX column separation showed that fraction F1-B, with the highest percentage of component A (Fig. 6c), possessed a higher G1 arrest-inducing activity than the F1 fraction (Fig. 6d). component A is relatively non-polar, and it is insoluble in $CHCl_3$, as indicated by a 90% purity through filtration of the organic fraction (fraction F1-In-1 in Fig. 6f) via the Bligh-Dyer method, followed by acetonitrile decantation (fraction F1-In-2). After conducting pyridine recrystallization (fractionF1-In-3), a 98% sample purity with 0.2% recovery was achieved (Fig. 6e, 6f) and this sample was then used for structure identification. The purification procedure is summarized in Fig. 6f. In brief, the active compound was successfully purified from the *Sanguisorba officinalis* extract by sequential application of the Bligh-Dyer method, acetonitrile decantation, and pyridine recrystallization.

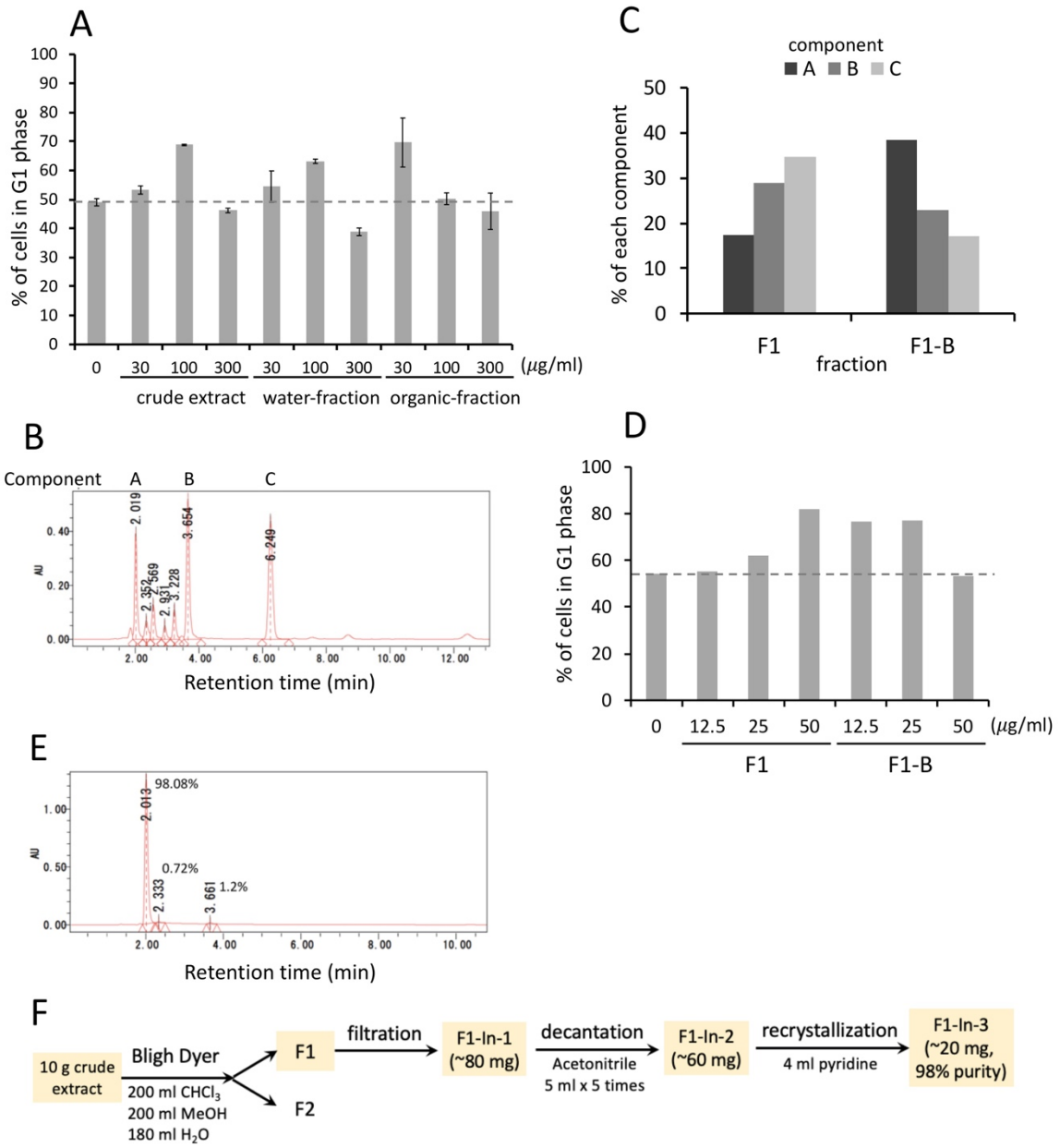

Fig. 6 Purification of the active compound in *Sanguisorba officinalis* extract

(a) Percentage of G1 cells after one day of the indicated treatments. Data are means ± SD, n=3.

(b) HPLC elution profile of Bligh-Dyer organic fraction (F1). Numbers on the peaks refer to the retention time of each compound.

(c) Percentages of the main components in the F1 fraction and the Oasis MAX column acidic buffer eluted fraction (F1-B) (basic compounds). A, B, C: main compounds in HPLC analysis (fig. 6b), with the retention time of A: 2.019 min, B: 3.654 min, C: 6.249 min.

(d) Percentage of G1 cells after a one-day treatment with the indicated concentrations of each fraction.

(e) HPLC elution profile of the compounds obtained from pyridine recrystallization (F1-In-3), labeled with the percentages of the total, based on the area under the curve of each peak. Numbers on the peaks show the retention time of each compound.

(f) Purification procedure with the relative amounts of samples and solvents. F1: organic-soluble fraction, F2: water-soluble fraction; F1-In: insoluble components in the F1 fraction.

3-4 The purified compound was identified as ellagic acid

The recrystallized sample was then characterized using ^{1}H-NMR (Fig. 7a), ^{13}C-NMR (Fig. 7b), FT-IR, and Mass Spectrometry. ^{1}H-NMR (400MHz, DMSO-d_6) δ 10.61 (bs,4H), 7.44 (s, 2H); ^{13}C-NMR (101MHz, DMSO-d_6) δ 159.39, 148.36, 140.02, 136.57, 112.58, 110.34, 107.65; The IR ATR spectrum showed peaks at 3475, 3154, 1721, 1617, 1322, 1261, 1108, 1037 cm^{-1}. The HR-MS (ESI) *m/z* was calculated the molecular formula for $C_{14}H_5O_8$ [M-H]- 300.9955; found 300.9974. The melting point was measured to exceed 350℃. From these results, ellagic acid (EA) was assumed to be the compound I purified from the *Sanguisorba officinalis* extract [44]. The chemical structure of EA is shown in Fig. 7c.

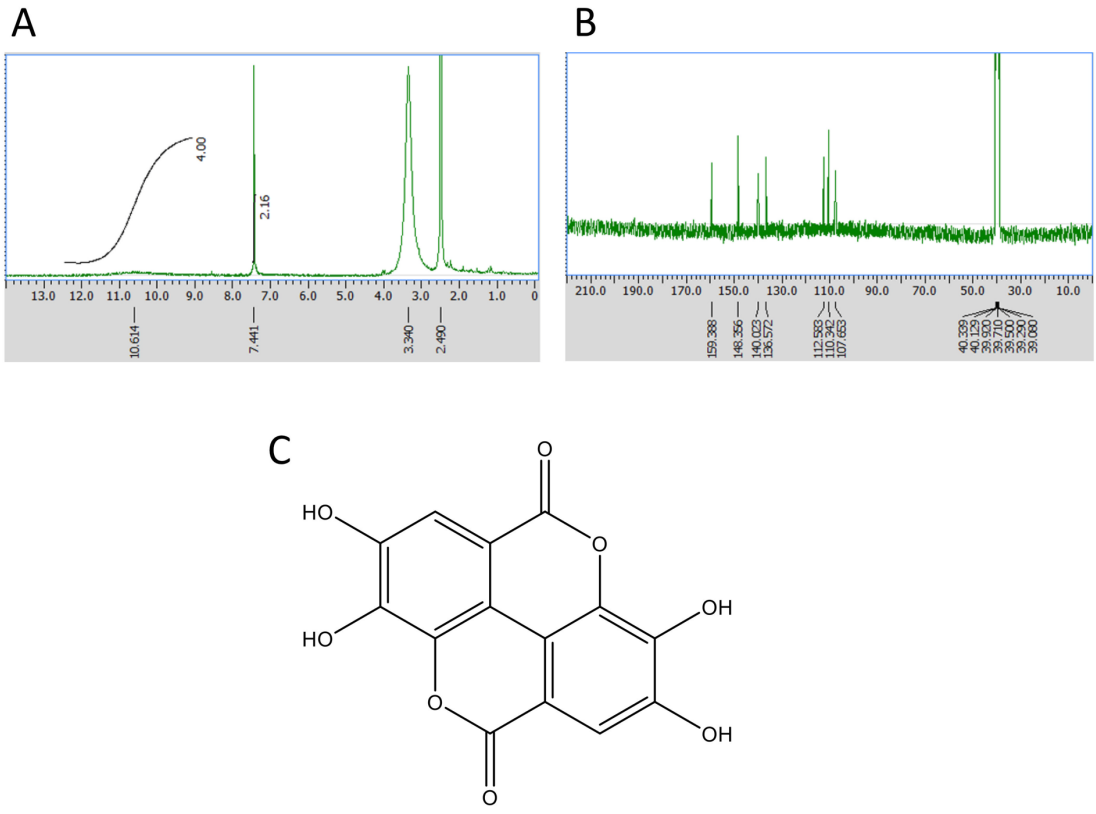

Fig. 7 Identification of the purified compound

(a,b) ^{1}H (a) and ^{13}C (b) NMR spectra of the purified compound. DMSO-d6 was used as the solvent. X-axis: chemical shift, ppm.

(c) The structure of ellagic acid, which was identified as the purified compound.

3-5 Ellagic acid is indeed the active compound inducing G1 arrest in the extract

Ellagic acid (EA) purified from *Sanguisorba officinalis* showed similar effectiveness in inducing G1 arrest in B16F10 with synthetic EA purchased from a commercial vendor. And both of them were significantly more effective than the crude extract (Fig. 8a).

To further confirm that EA is indeed the active compound in the extract, HPLC analysis of the *Sanguisorba officinalis* extract was conducted (Fig. 8b), and the component released at 2.029 min is inferred to be EA. The weight ratio of EA in *Sanguisorba officinalis* extract was calculated to be 0.049 ± 0.015 (n=3). Namely, 100 μg/ml crude extract contained 4.9 μg/ml (16.3 μM) EA, which is sufficient for inducing G1 arrest (Fig. 8a, 10b) in B16F10 cells.

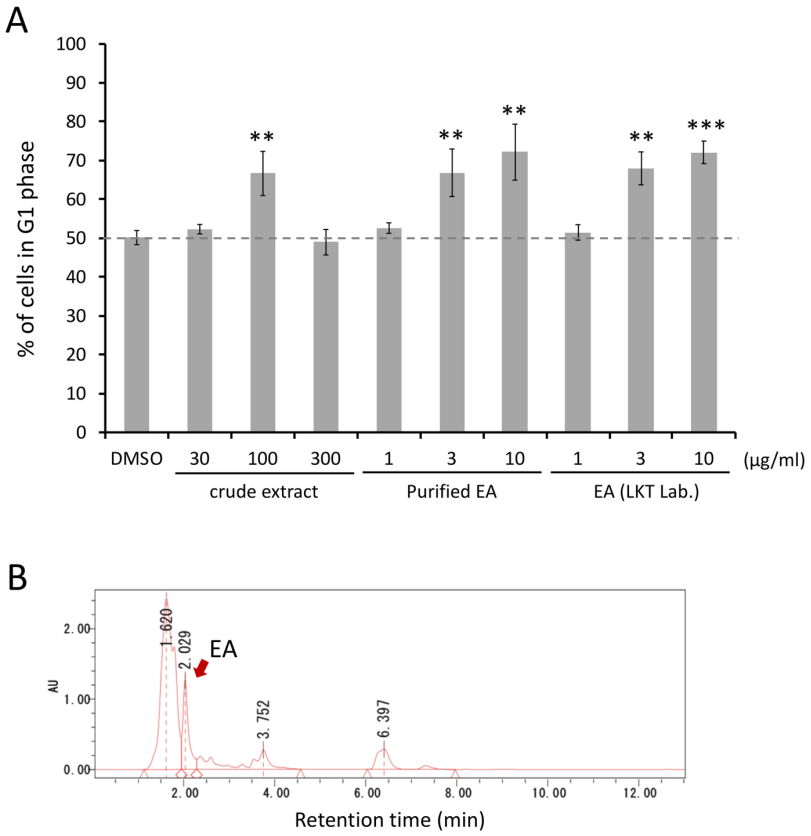

Fig. 8 Ellagic acid is indeed the compound responsible for inducing G1 arrest in the extract

(a) Percentage of cells in G1 phase after 24 hr indicated treatments. EA (LKT lab.): ellagic acid powder purchased from LKT Laboratories, Inc. Data are means ± SD. Student's t-test: **: $p < 0.01$, ***: $p < 0.001$.

(b) HPLC elution profile of *Sanguisorba officinalis* extract. Numbers on the peaks refer to the retention time.

3-6 The anti-proliferation effect of EA is time- and dose-dependent

EA is a polyphenol found in many plants and is known for harboring liver-protection, melanogenesis inhibition activities [45-48]. Previous studies also showed that EA induces cell cycle arrest, cell death through modulating NF-κB, PI3K/Akt, TGF-β/Smad3 pathways in many cancer cell lines [49-51]. However, its effects on melanoma cells and the key mechanism are still unknown.

I then further characterized the effects of pure EA on B16F10 cells. B16F10 cells were incubated with varying concentrations of EA for 1-3 days (Fig. 9a). Cell morphology began to change on day 1 (Fig. 9b) but significant differences in cell numbers were not observed at that time (Fig. 9d). Dose-dependent growth inhibition was observed on day 2 and day 3 (Fig. 9c, 9d).

After 2 days of treatment with either 20 or 30 μM EA, a population of subG1 cells was prominent (Fig. 9f), and on day 3 of treatment, the percentage of subG1 cells became even greater (Fig. 9e, 9f). Also, 30 μM EA treatment induced more cell death than the 20 μM EA treatment (Fig. 9e, 9f). These results demonstrate that EA treatment inhibits B16F10 cell proliferation and induces cell death in a time- and a dose-dependent manner.

Fig. 9 Cell toxicity caused by EA is dose and time dependent

(a) The experimental procedure, orange line indicates the drug-treatment duration and the blue one indicates time without any treatment.

(b, c) B16F10 cell morphology after 1 day (b) and 2 days (c) of treatment with EA at the indicated doses.

(d) Relative living cell numbers after EA treatments (μM) compared to day 0, the time point for the addition of drugs. Data are means ± SD, n=3. Student's t-test, *: $p < 0.05$, **: $p < 0.01$.

(e) Cell cycle profiles based on PI fluorescence intensity after 3 days of EA treatment at the indicated concentrations.

(f) Percentage of subG1 cells estimated by FACS analysis. Concentration unit: μM. Data are means ± SD, n=3. *: $p < 0.05$, **: $p < 0.01$, ***: $p < 0.001$ in Student's t-test.

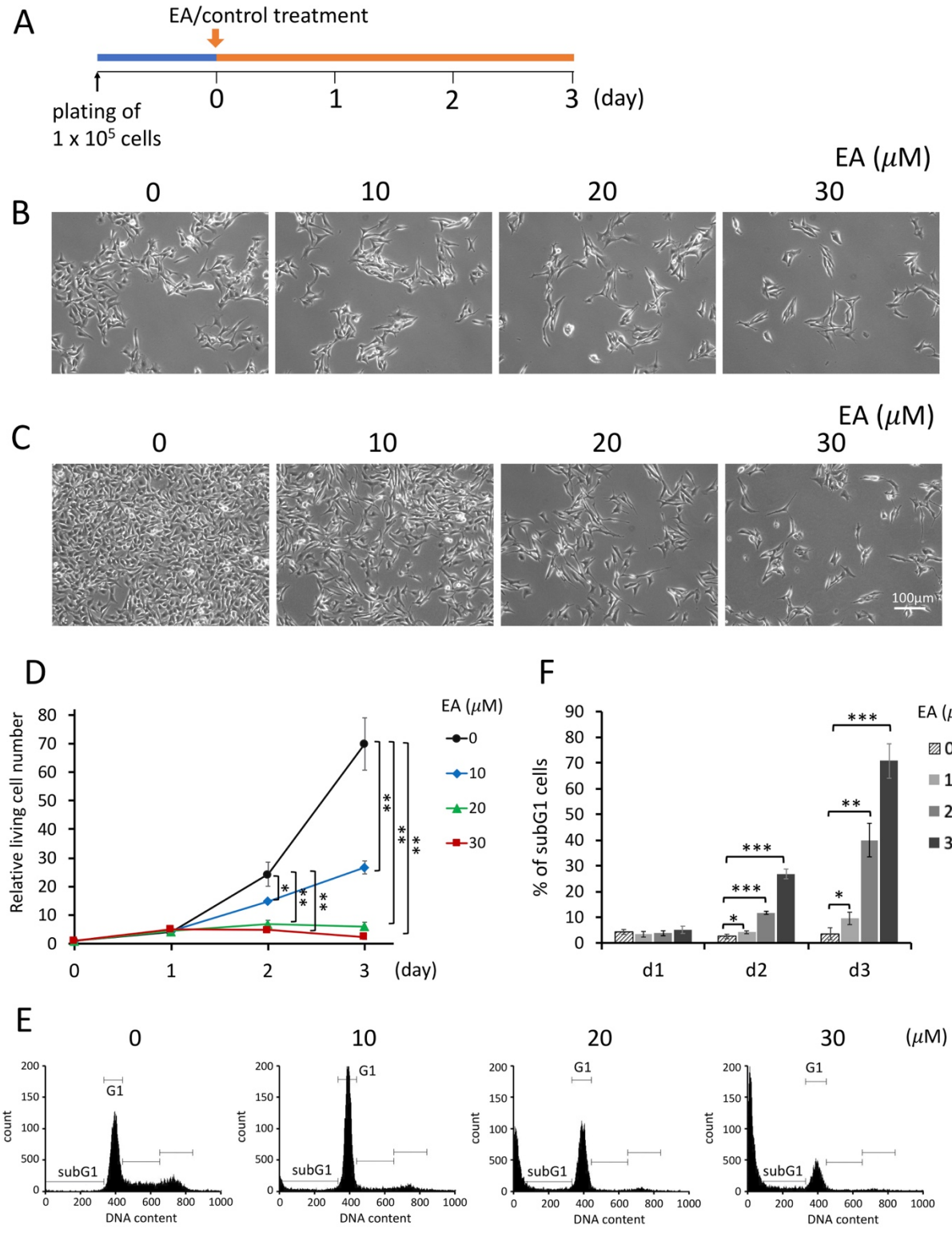
A
EA/control treatment
plating of
1 x 10^5 cells
0
1
2
3
(day)
B
EA (μM)
0
10
20
30
C
EA (μM)
0
10
20
30
100μm
D
Relative living cell number
EA (μM)
0
10
20
30
(day)
F
% of subG1 cells
EA (μM)
d1
d2
d3
E
0
10
20
30
(μM)
G1
subG1
count
DNA content

Figure 9

3-7 EA induced G1 Arrest in a dose-dependent manner

Next, to examine the effects of EA on the cell cycle, flow cytometry was conducted. A 24 hr treatment with 20 μM EA resulted in 85% of the cells accumulating in G1 phase; and a 24 hr treatment with higher concentration (30 μM) of EA did not lead to a further accumulation in G1 phase (Fig. 10a, 10b). The percentages of G1 cells within living cells showed similar patterns in treatments with increasing exposure times (Fig. 10c). The results in 3-6 and 3-7 clearly demonstrate that EA treatment induces G1 arrest in a dose-dependent manner at relatively low concentrations, and elicits cell death as the duration or the concentration of the treatment increases.

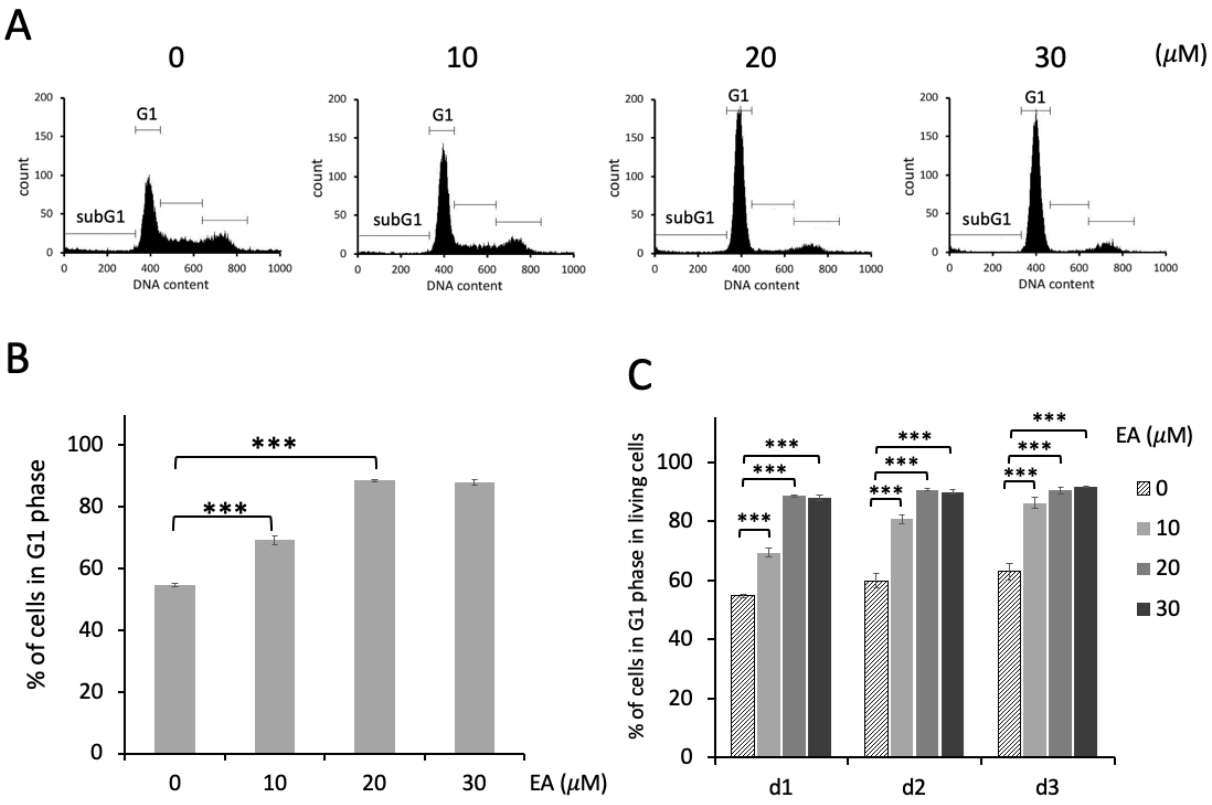

Fig. 10 EA causes dose-dependent G1 arrest in B16F10 cells

(a) Cell cycle profiles based on PI fluorescence intensity after 24 hours of EA treatment at the indicated concentrations.

(b) Percentage of G1-phase cells after 24-hour treatment. Data are means ± SD, n=3. Student's t-test: ***: $p < 0.001$.

(c) Percentage living cells in G1 phase, determined by FACS analysis. Concentration unit: μM. Data are means ± SD, n=3. Student's t-test: ***: $p < 0.001$.

3-8 EA affects AKT, MAPK activities and p53 protein levels in B16F10 cells

MAPK and AKT signaling pathways, which play important roles in promoting cell growth and survival, are often excessively activated in melanoma cells through *N-RAS*, *BRAF,* or *PTEN* mutations [52-54]. Moreover, some previous studies indicated that EA is related to the modulation of the MAPK and AKT signaling networks [49,55]. Also, EA somehow causes increment of p53 protein levels in some cancer cell lines [56].

After a 24-hour treatment, EA reduced the phosphorylation levels of AKT, its downstream effector p70S6K (Fig. 11a), and p44/42 MAPK (Erk1/2) (Fig. 11b) in B16F10 cells. Since phosphorylation of these kinases is indispensable for their biological activities [57-59], EA treatment leads to the diminished capacity to activate these cell growth-promoting signaling pathways. Additionally, p53 and p21 protein levels increased (Fig. 11c). All these effects were positively correlated with the EA concentration.

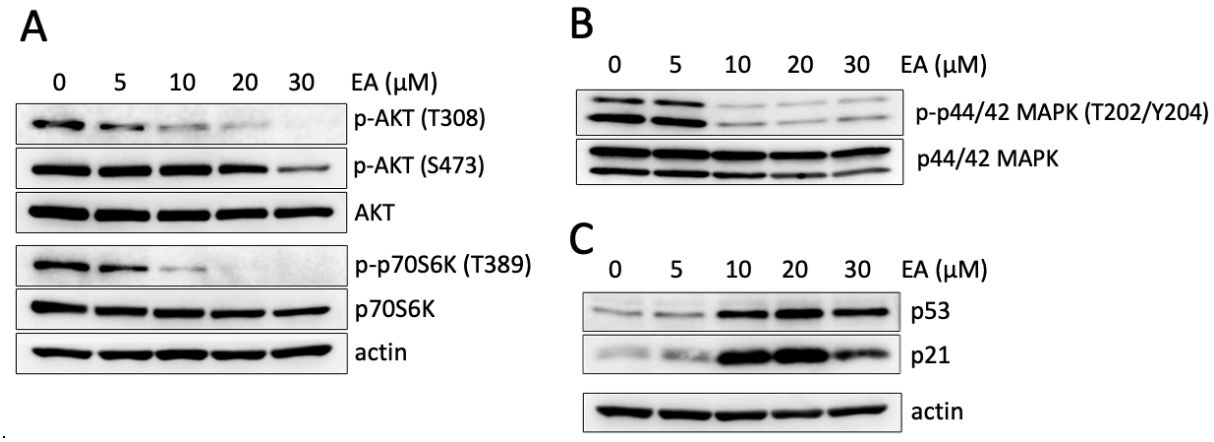

Fig. 11 EA attenuates cell growth related signaling pathways and increases p53 protein levels
(a-c) Western blot analysis of growth factor stimulated signaling pathway activation (a, b) and protein levels of p53, p21 (c). Lysates from B16F10 cells were collected after 24 hours, with the indicated treatments. Actin is shown as the loading control.

3-9 EA did not appear to inhibit CK2 activity

In order to find targets of EA, I first investigated the molecules related to p44/42 MAPK, AKT, and p53 modulation. Casein kinase 2 (CK2) has been reported for its multiple roles affecting numerous pathways within a cell, including the activities of both MAPK and AKT signaling and p53 stability [60-63]. A previous study suggested EA as a potential inhibitor of CK2 [64]. CK2 is a serine/threonine protein kinase targeting multiple substrates, and thus I examined the phosphorylation levels of CK2 substrate motifs as indicators of its activity. Compared to DMSO (vehicle) treatment, no any suppression of phosphorylation levels in potential CK2 targets was observed in EA treatment (Fig. 12), implying that CK2 is not likely a target of EA regarding the phenotypes observed in B16F10 cells.

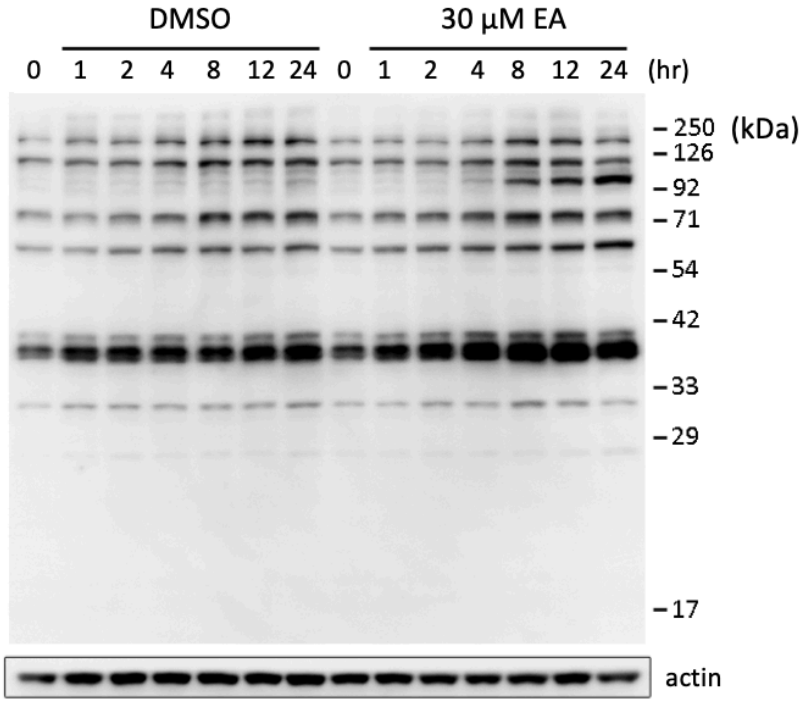

Fig. 12 CK2 inhibition is not the primary effect of EA

After time variable treatment of B16F10 cells with 30μM EA, phosphorylation levels of CK2 substrates were detected by Immuno-blotting with a phospho-CK2 substrate motif [(pS/pT)DXE] antibody.

3-10 An increase in p53 protein was the earliest event observed in EA treatment

Next, to narrow down EA targets to a small number of candidates, time-course experiments were performed on the supposition that the molecule more closely related to EA target may show difference earlier than its downstream effectors. Cells were collected at various time points after the initiation of EA treatment to a final concentration of 30 μM, and phosphorylation/protein levels were measured by western blotting. Significant declines of AKT Thr308 and Ser473 phosphorylation were observed after a 24-hour treatment with EA (Fig. 13a, 13b). Regarding the phosphorylation levels of p44/42 MAPK on T202 and Y204, EA treatment appeared to dampen the phosphorylation (Fig. 13c), but the variations among the experiments were too large to unambiguously express significant differences between EA and control treatments (Fig. 13d). The earliest event that I observed was an increment in the level of p53 protein, which started as early as 2 hours after the EA addition, and became significantly elevated 4 hours after the treatment (Fig. 13e, 13f). It is notable that an elevation in the level of p21 protein, a p53 transcriptional target, followed the rising in the p53 protein level (Fig. 13e). From these results, I assumed that increase in p53 level is the cause of G1 arrest and other phenotypes.

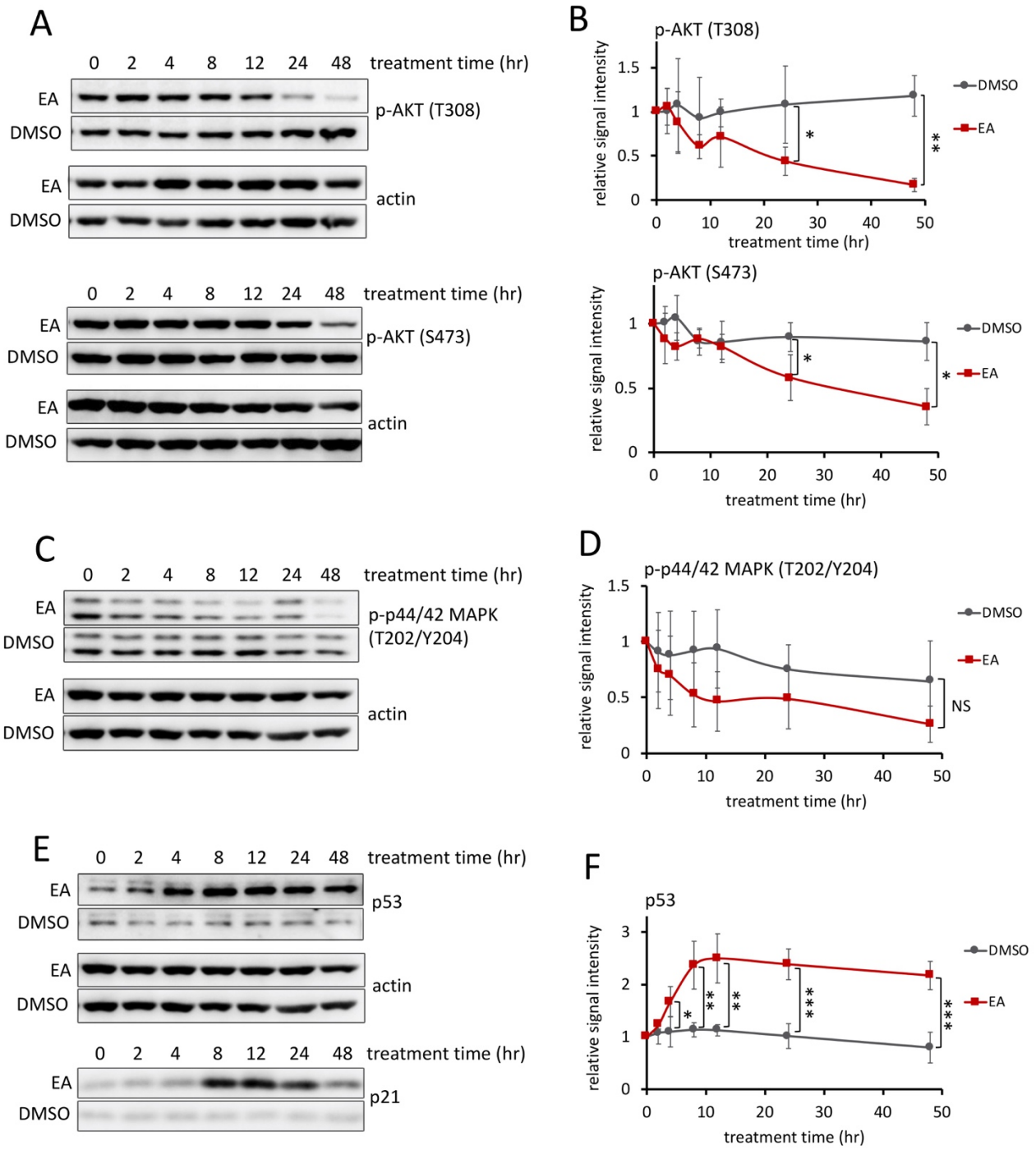

Fig. 13 Time course experiments showed p53 accumulation as the earliest event in EA treatment
(a, c, e) Time courses of the indicated proteins/phosphorylations from B16F10 cell lysates collected after indicated duration of treatments with DMSO control or 30 μM EA, analyzed by western blotting. (b, d, f) Relative protein/phospho-protein amounts normalized to the 0 hr time point (adding treatments) for each respective treatment. DMSO: 0.5% DMSO solvent control, EA: 30 μM. (b, d) n=3. (f) n=4. *: $p < 0.05$, **: $p < 0.01$, ***: $p < 0.001$, NS: non-significant in student's t-test.

3-11 p53 increment is not the cause of other phenotypes

Subsequently, I examined whether the elevated p53 protein amount is causative for the G1 arrest as well as the other phenotypes. To know the answer, B16F10 cells were treated with EA and variable concentrations of Pifithrin-α-HBr, a p53 inhibitor[65] , simultaneously. As I expected, pifithrin-α-HBr treatments repealed the EA-induced elevation in the levels of p21 and cyclin D1 proteins (Fig. 14a), both of which are transcriptional targets of p53. However, the p53 inhibitor did not affect the EA-induced reduction of AKT phosphorylation; nor did they influence the EA-induced attenuation in p70S6K phosphorylation, a downstream effector of AKT signaling pathway (Fig. 14a). With respect to G1 arrest, pifithrin-α-HBr treatments failed to reverse the EA-induced G1 arrest, as might be expected with p53 inhibition (Fig. 14b). Rather, pifithrin-α-HBr treatments by themselves induced G1 arrest (Fig. 14c). Taken together, these results exclude the possibility that p53 activity is essential for inactivation of the AKT signaling pathway as well as for inducing G1 arrest in response to the EA treatment.

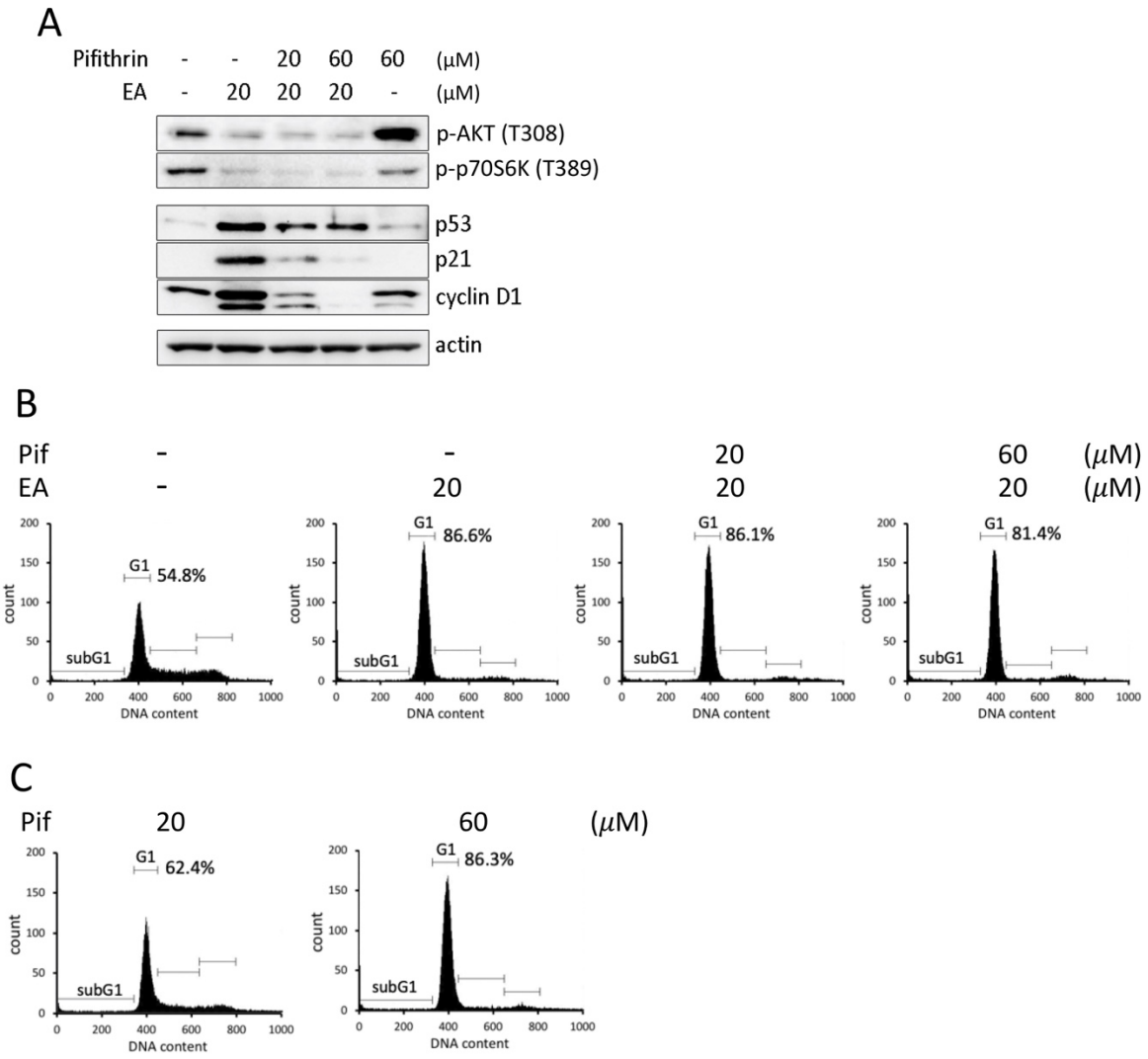

Fig. 14 p53 upregulation is not the primary effect of EA

(a) Protein levels of p53, p21, cyclin D1, and the phosphorylation levels of AKT (T308) and p70S6K (T389) were detected by Western blotting following 24-hour EA/p53 inhibitor Pifithrin-α-HBr treatments.

(b, c) Cell cycle profiles after 24 hours of each respective treatment. The number in each plot indicates the relative abundance of G1-phase cells among the entire population. EA concentration: 20 μM. Pif: pifithrin-α-HBr.

3-12 Inhibition of PTEN reversed all the EA-induced phenotypes in B16F10 cells

It is known that activated PI3K phosphorylates PIP2 into PIP3, which in turn stimulates downstream signaling modules, such as PDK1 and AKT [8]. And PTEN plays an opposing role, converting PIP3 into PIP2 [14]. In order to reactivate AKT signaling in EA treatments, increasing concentrations of VO-OHpic trihydrate, a PTEN specific phosphatase inhibitor [66], were added to the cells combined with EA. Surprisingly, all of the EA-induced effects--G1 arrest (Fig. 15a, 15b) as well as declined phosphorylations of AKT (both at Thr308 and Ser473), p70S6K (at Thr389), and even p44/42 MAPK (at Thr202/Y204) (Fig. 15c)--were reversed by the addition of VO-OHpic trihydrate in a dose-dependent manner. VO-OHpic trihydrate treatment alone appeared to affect neither the cell cycle (Fig. 15a) nor the cell morphology (Fig. 15d), suggesting that the reversal of the cell cycle arrest was possibly achieved by counteracting the effect of EA. Furthermore, addition of VO-OHpic trihydrate reversed the anti-proliferation effect of EA in a dose-dependent manner (Fig. 15d, 15e). These data demonstrate that PTEN phosphatase activity is indispensable for the EA-induced phenotypes. This in turn raised the possibility that EA contributes to PTEN activation.

Fig. 15 Inhibition of PTEN reverses the phenotype induced by EA treatment

(a) FACS-based cell cycle profiles based on PI fluorescence intensity after 24 hr treatments of EA /VO-OHpic trihydrate (VO) or combinations of both compounds. EA concentration: 20 μM. VO-OHpic trihydrate concentration: 4 μM.

(b) Percentage of cells in G1 phase, determined by FACS analysis after 24 hr treatments with 20 μM EA combined with increasing concentrations (1, 2, 4 μM) of VO-OHpic trihydrate (VO). Data are means ± SD, n=3. **: $p < 0.01$, *** $p < 0.001$ in student's t-test.

(c) Western blots with indicated antibodies after 24 hr treatments with 20 μM EA, VO-OHpic trihydrate, or combinations of both compounds. Concentrations of VO-OHpic trihydrate: 1, 2, 4 μM.

(d) Cell morphology after 24 hr of each respective treatment.

(e) Relative living cell numbers after 48 hr treatment with 20 μM EA and various concentrations (1, 2, 4 μM) of VO-OHpic trihydrate. Data are means ± SD, n=3. Student's t-test, **: $p < 0.01$, ***$p < 0.001$.

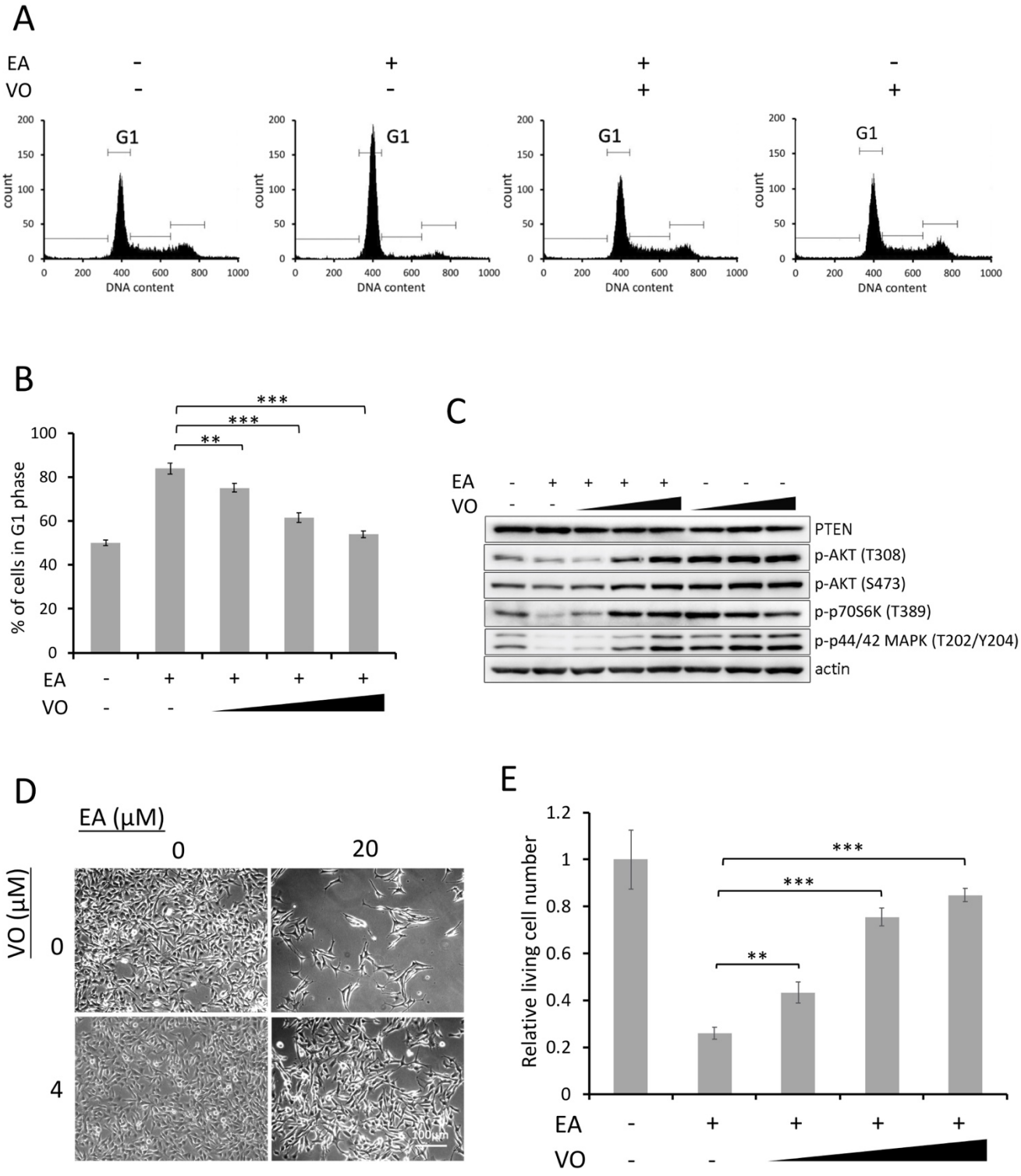
A
EA - + + -
VO - - + +
G1
count
DNA content
B
% of cells in G1 phase
***
***
**
EA - + + + +
VO - - ▲
C
EA - + + + + - - -
VO - - ▲ ▲
PTEN
p-AKT (T308)
p-AKT (S473)
p-p70S6K (T389)
p-p44/42 MAPK (T202/Y204)
actin
D
EA (μM)
0
20
VO (μM)
0
4
100μm
E
Relative living cell number
***
***
**
EA - + + + +
VO - - ▲

Figure 15

3-13 The PI3K inhibitor LY294002 showed different effects from EA

Although I favored my hypothesis that EA enhances PTEN activity, it's necessary to inquire into the possibility that EA works as a PI3 kinase inhibitor, since the activation of AKT is a result of the balance of PI3K and PTEN activities. To discern which is the EA mechanism, I checked the effects of LY294002, a well-used PI3K inhibitor [67], in B16F10 cells. As expected, an apparent immediate decrease of AKT phosphorylation, as early as 2 hr after the LY294002 treatment, was observed (Fig. 16a). However, at later timepoints (24 hr to 48 hr) the phosphorylation levels of AKT were restored or even enhanced (Fig. 16a), quite different from EA properties (i.e., slow, but sustained inhibition (Fig. 13a)). The combination of EA with LY294002 prevented the slow restoration of AKT phosphorylation (Fig. 16b), implying that EA may not act on PI3K as LY294002 does. More importantly, the sustained p53 accumulation observed with EA treatment (Fig. 13e) was not observed with LY294002 treatment (Fig. 16c). Moreover, the time-course data of EA treatment showed that the increment in the p53 level occurred much earlier than the onset of AKT dephosphorylation (Fig. 13). Consequently, it is not likely that AKT inactivation resulted in upregulation of p53. Previous studies showed that PTEN directly interacts with p53, enhancing its stability and causing increased p53 levels and activity [68]. These observations and the previous results collectively support the idea that rather than PI3K, PTEN is more likely the target of EA.

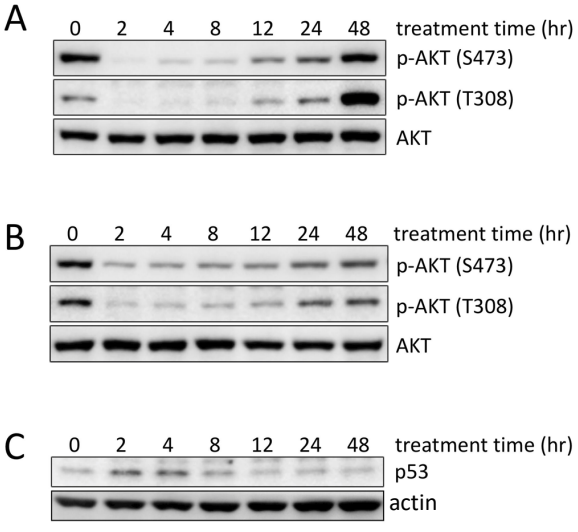

Fig. 16 EA showed different effects from the PI3K inhibitor

(a-c) Immunoblot analysis of AKT protein signaling activation (a,b) and protein levels of p53 (c) in a time course of 30 μM LY294002 treatment (a,c) or a combination of 30 μM LY294002 and 30 μM EA (b).

3-14 EA treatment affects PTEN activities in B16F10 Cells

Based on my observation that a PTEN inhibitor reversed the EA activity, EA probably causes an overall increase in PTEN activity, meaning that either an increase in the total PTEN protein amount or PTEN activation, or both, are possible mechanisms. First, PTEN protein levels were measured at various time points after the initiation of EA (30 μM) treatment. However, no difference was observed up to 24 hours of treatment between control and EA treatments (Fig. 17a, 17b). Therefore, I next examined the effect of EA on PTEN activity. It is known that PTEN harbors both lipid phosphatase activity and protein phosphatase activity [69]. FAK is a well-defined PTEN protein substrate [70], and its dephosphorylation leads to inactivation of its downstream targets, including the PI3K-AKT signaling pathway [70,71]. PTEN is also known to dephosphorylate Shc, which, in turn, inactivates RAF-MEK-p44/42 MAPK[72] pathway. What's more, PTEN interacts with p53, leading to p53 stabilization [68]. Combining these lines of evidence with my observations, I anticipated that an upregulation in protein phosphatase activity of PTEN is a key mechanism of EA action. Therefore, I performed experiments monitoring the phosphorylation levels of FAK in Tyr397 (PTEN dephosphorylation site) after time-variable treatments of EA, and observed that EA treatment resulted in decreased FAK phosphorylation, and VO-OHpic trihydrate prevented the attenuation (Fig. 17c, 17d). No change was found in the total amount of FAK protein (Fig. 17c). Moreover, a transitory increase in p53 protein levels, which was observed with EA treatment, was also eliminated by the VO-OHpic trihydrate (Fig. 17e, 17f). Treatment of B16F10 cells with VO-OHpic trihydrate alone did not affect phosho-FAK or p53 levels (Fig. 17c, 17e). In conclusion, these results support my idea that EA causes an enhancement in PTEN protein phosphatase activity.

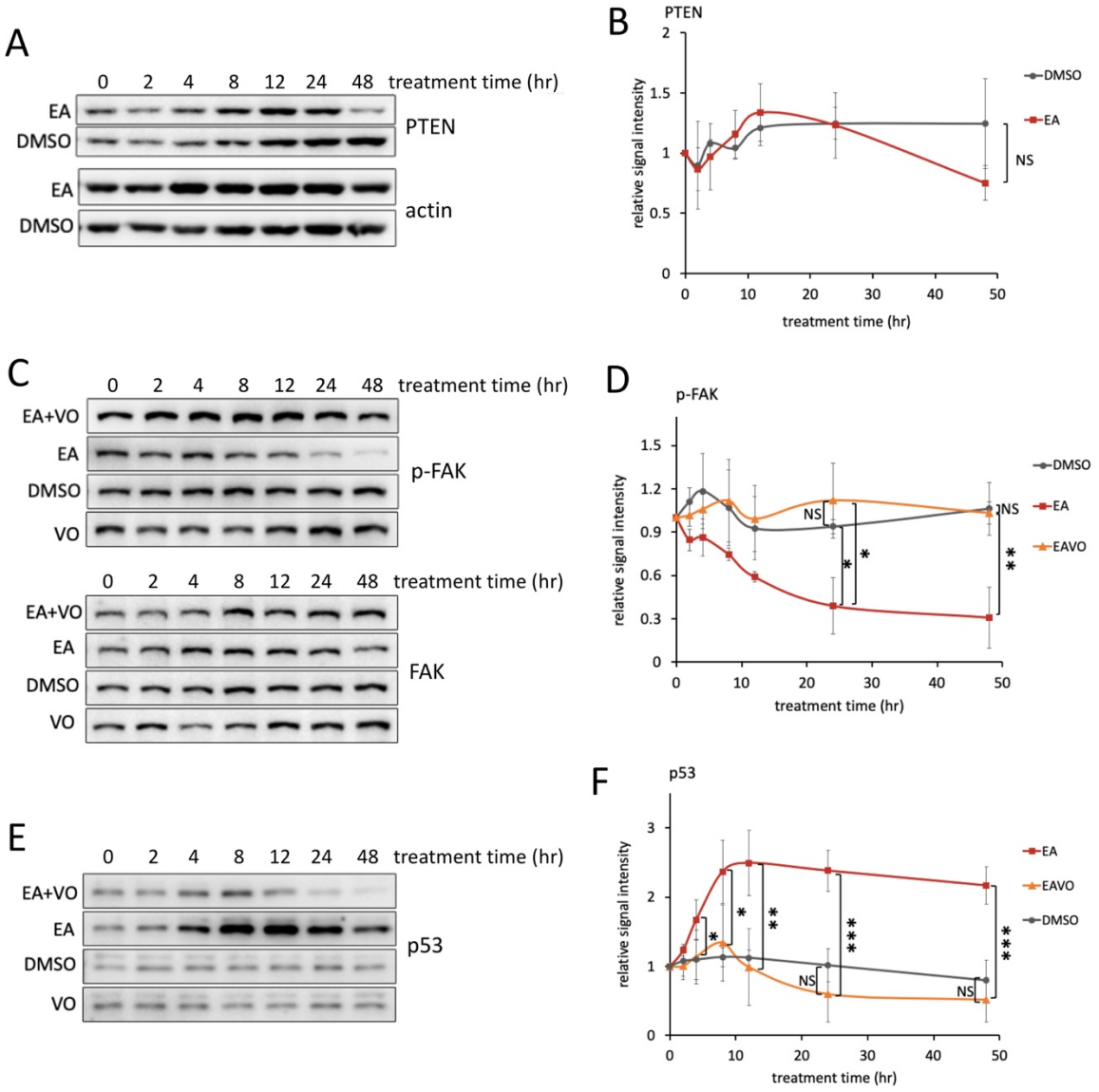

Fig. 17 EA treatment affects PTEN activities in B16F10 cells

(a, c) Western blot of PTEN (a), phospho-FAK and FAK (c), after the indicated duration of treatments. Actin is shown as the loading control. EA+VO: the combination of 30 μM EA and 4 μM VO-OHpic trihydrate; EA: 30 μM ellagic acid; DMSO: 0.5% DMSO control; VO: 4 μM VO-OHpic trihydrate.

(b, d) Relative PTEN (b) and phospho-FAK (d) amounts normalized 0 hr time point (adding treatments) for each respective treatment. EAVO: the combination of 30 μM EA and 4 μM VO-OHpic trihydrate; EA: 30 μM ellagic acid; DMSO: 0.5% DMSO control. n=3. *: $p < 0.05$, **: $p < 0.01$. NS: non-significant in Student's t-test.

(e) Immuno-blotting time course of p53 protein after the indicated treatments. EA+VO: the combination of 30 μM EA and 6 μM VO-OHpic trihydrate, EA: 30 μM EA, DMSO: 0.5% DMSO solvent control.

(f) Relative p53 protein amounts, normalized to the 0 hr timepoint, after the indicated treatments. EA: 30 μM EA, EAVO: the combination of 30 μM EA and 6 μM VO-OHpic trihydrate, DMSO: 0.5% DMSO control. n=4. Student's t-test, *: $p < 0.05$, **: $p < 0.01$, ***: $p < 0.001$

3-15 EA directly modulates the PTEN phosphatase activity

To further confirm that EA is directly related to PTEN activity, an *in vitro* analysis of PTEN lipid phosphatase activity was performed. The activity assays showed that EA directly modulates the PTEN phosphatase activity; namely, EA inhibited PIP3 conversion to PIP2 in a dose-dependent manner (Fig. 18a). Differ from the observation in cell culture, the addition of VO-OHpic trihydrate with EA resulted in further inhibition of PTEN lipid phosphatase activity (Fig. 18b). This result excluded the concern that VO-OHpic trihydrate directly captures EA and compensates its function. Furthermore, EA partially counteracted the effects of the PI3K inhibitor at earlier time points (Fig. 16a and 16b), meaning that EA and PI3K inhibitor may play opposite roles in PIP2-PIP3 conversion. The results in 3-14 and 3-15 collectively suggest that EA functions as an allosteric modulator of PTEN, enhancing its protein phosphatase activity while inhibiting its lipid phosphatase activity (Fig. 19).

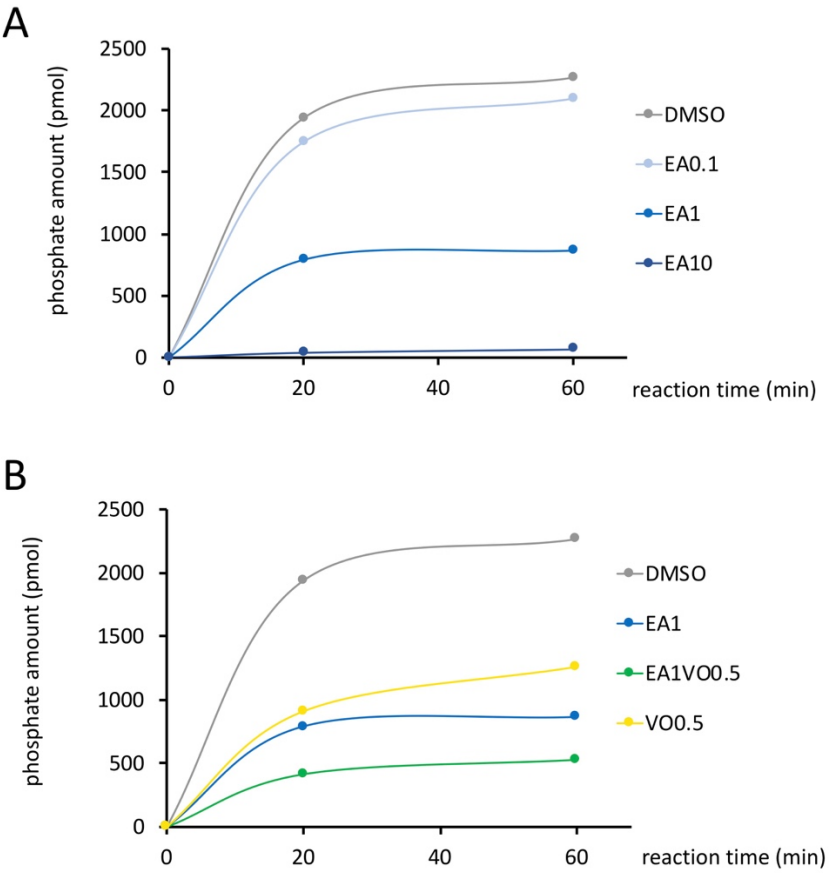

Fig. 18 EA directly modifies the PTEN phosphatase activity

(a, b) In vitro analysis of recombinant PTEN activity. 3000 pmol PIP3 was added to each reaction with the indicated compounds (μM). Phosphate amount (pmol) was calculated by Malachite Green assay at 20 and 60 min timepoints. n=2.

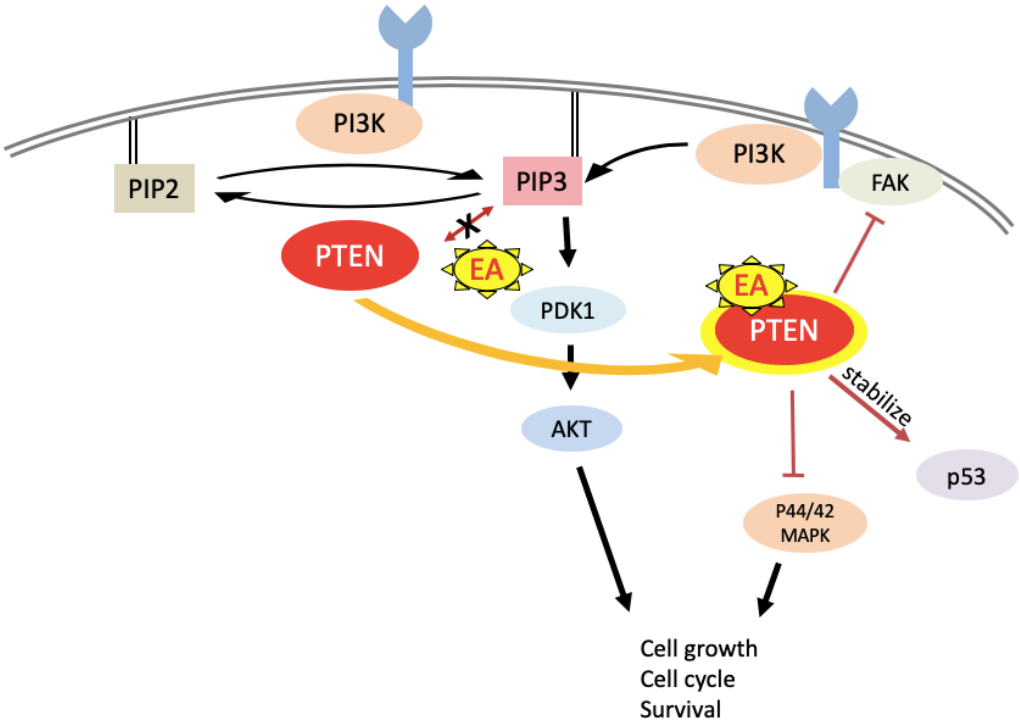

Fig. 19 Schematic illustration of the proposed EA function

EA enhances PTEN protein phosphatase activity whereas abrogates its lipid phosphatase activity, and thus, is supposed to be an allosteric modulator of PTEN.

3-16 Combination treatment of EA and cisplatin in B16F10 cells

Inhibition of AKT-related signaling pathways is generally applied as a strategy for impeding cancer cell growth [8]. Unluckily, most of the time, re-activation of AKT is observed through a feedback mechanism that cells are able to conquer the unfavorable circumstances of PI3K inhibition, thus limiting the application of PI3K inhibitors in the clinical treatments[73,74]. In my experiments, re-elevation of phospho-AKT was also observed in B16F10 cells after 48 hours of adding PI3K inhibitor LY294002 (Fig. 16a). On the other hand, EA provided quite different profiles in impeding AKT activation, namely a slow, prolonged decline in AKT phosphorylation (Fig. 13a). These results raised the possibility that EA could inhibit AKT

activity in cancer cells without the re-activation of AKT, as observed in PI3K inhibitor treatment, proposing that a combination treatment of EA with a general antiproliferative chemotherapeutic drug would possibly provide a new anti-cancer strategy with great efficacies.

Cisplatin is a chemotherapy agent used to treat kinds of cancers including lung cancer, ovarian cancer, testicular cancer, et cetera[75]. It is known to cause DNA damage in treated cells [75]. To reduce the risk of drug resistance and adverse side effects, combination therapy with other agents to lower concentration of cisplatin is recommended [75,76]. The AKT signaling pathway has been suggested to contribute to the protection of cells from death during cisplatin treatment [75,76]. I thus assumed that EA treatment, which weakens AKT signals, would induce strong anti-proliferative effects in conjugation with cisplatin.

The experimental procedure is shown in Fig. 20a. Indeed, the combination treatment of EA and cisplatin strongly inhibited cell proliferation and induced much more pronounced cell death (Fig. 20b). B16F10 cells arrested the cell cycle in G2 phase when incubated with cisplatin alone (Fig. 20c). In contrast, about 80% cells were dead (subG1 population in FACS analysis/ trypan blue assay) 3 days after the combined treatment (even 2 days after the removal of the drugs) (fig. 20c, 20d). The cell death was much more conspicuous with the combined treatment than with either of the single drug treatments. I then traced the living cell numbers for longer time periods to see whether the cells started to re-grow after the cessation of the treatment. In 1 week after removal of drugs, living cell numbers were still declining in the combination treatment (Fig. 20e), indicating that the cells are still engaged in the cell death program even after the removal. In this process, EA with cisplatin more effectively reducing phosphorylation level of AKT and its downstream effector p70S6K (Fig. 20f). These results propose that EA and cisplatin have a synergistic effect in inducing cell death in B16F10 melanoma cells, providing a possible application in novel cancer therapeutic strategy.

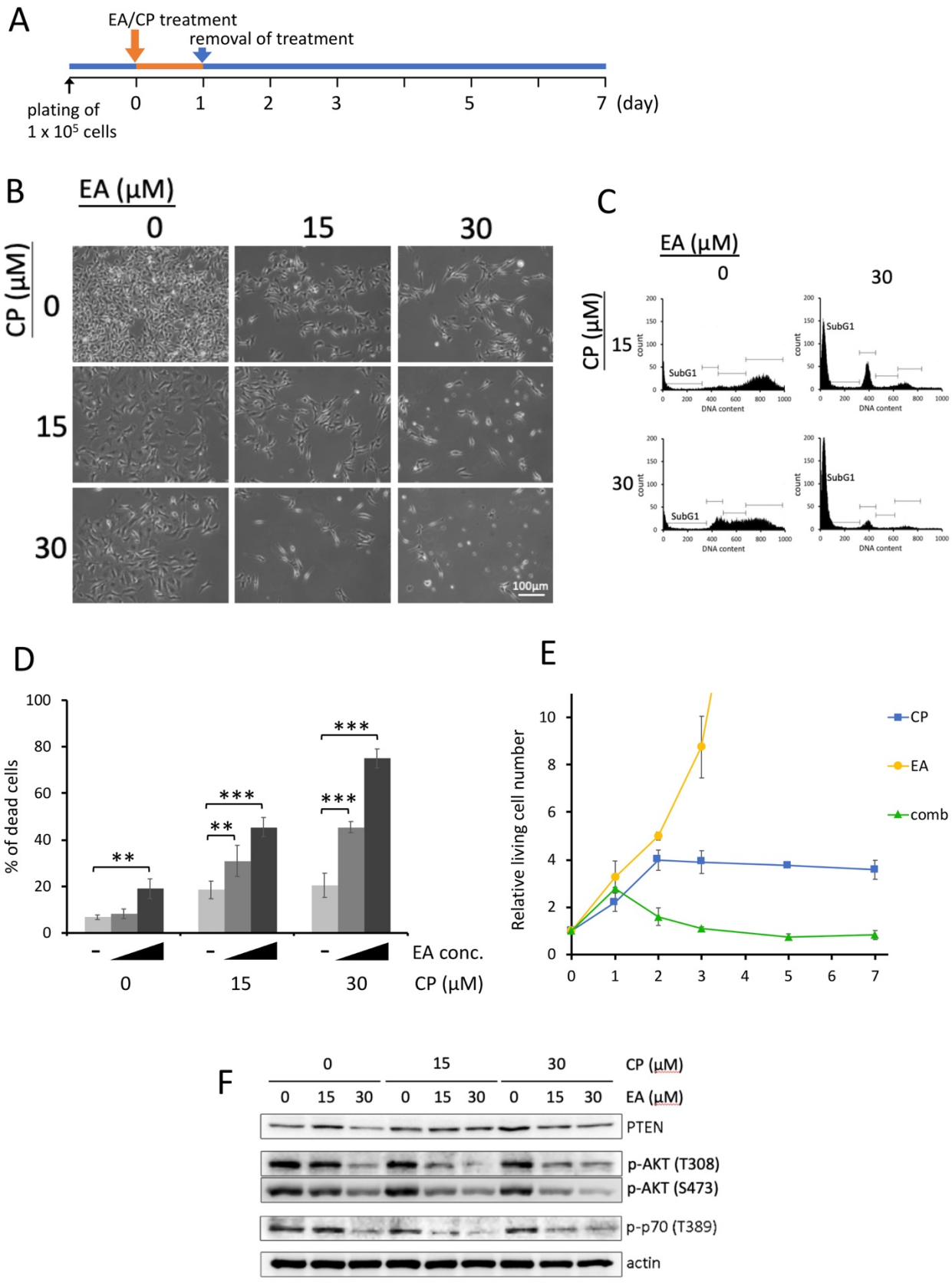
A
EA/CP treatment
removal of treatment
plating of
1 x 10^5 cells
0
1
2
3
5
7 (day)
B
EA (μM)
0
15
30
CP (μM)
0
15
30
100μm
C
EA (μM)
0
30
CP (μM)
15
30
SubG1
count
DNA content
D
% of dead cells
100
80
60
40
20
0
**
***
EA conc.
CP (μM)
E
Relative living cell number
CP
EA
comb
F
CP (μM)
EA (μM)
PTEN
p-AKT (T308)
p-AKT (S473)
p-p70 (T389)
actin

Figure 20

Fig. 20 Combined treatment of EA and cisplatin effectively causes cell death in B16F10 cells

(a) The experimental design: orange line indicates the drug-treatment duration, and blue one represents absence of drug exposure. CP, cisplatin.

(b) Cell morphology with the indicated combination of treatments on day 2 (one day after the removal of the compounds).

(c) Cell cycle profiles based on PI fluorescence intensity of cells collected on day 3 of treatment with DMSO control, 30 μM CP (cisplatin), 30 μM EA, or in combination of the both.

(d) Percentage of dead cells in a trypan blue assay. Cells were collected on day 3 (two days after removal of the compounds). EA concentration: 15, 30 μM. Data are means ± SD, n=4. Student's t-test, **: $p < 0.01$, ***: $p < 0.001$.

(e) Relative living cell numbers compared to day 0, the time point for the initiation of drug treatment. Cells were treated with 30 μM cisplatin, 30 μM EA, or the combination for 1 day and then the treatments were halted by replacing the medium with fresh medium lacking EA and cisplatin. Data are means ± SD, n=3.

(f) Western blot analysis of protein phosphorylation after 24 hr treatments, as indicated.

4. Discussion

The inhibition effect of *Sanguisorba officinalis* extract in tumor growth has been demonstrated in numbers of cancer cell lines. Though numerous studies have described the purification procedures and identification of effective compounds, only a few studies identified ellagic acid (EA) or EA-derived compounds as the responsible ingredient [40,77,78]. Also, this is the first report identifying EA as the G1-arrest inducing compound in *Sanguisorba officinalis* extracts. It is notable that this study outlines a simplified and practical method for extracting EA from *Sanguisorba officinalis* without using any column chromatography. EA is already marketed as a health supplement (antioxidant) or skin whitener, and there seem to be few side effects, if any, in healthy people. However, EA is very expensive. My simple method could not only shorten the operation time but also lower its price.

Both EA and *Sanguisorba officinalis* extracts were able to cause anti-proliferative effects with G1 arrest phenotypes in a dose- and a time-dependent manner. The quantification result of EA amount in the extract also suggests that these effects were mostly due to the presence of EA. Together with the results of the *in vitro* experiment, in which EA directly inhibited the PTEN lipid phosphatase activity, I posit that EA works as an allosteric regulator of the PTEN protein phosphatase activity. The EA-bound PTEN protein, with a dampened lipid phosphatase activity, may have the tendency to bind to and dephosphorylate its target protein substrates, such as FAK. Still, my *in vitro* experiments could not completely rule out the possibility that EA may activate/inhibit a yet-unidentified PTEN regulator in the cells. Further investigation would be required to exclude this possibility. Also, examinations of how PTEN exactly behaves in the present of EA, for example, the interaction with its substrate proteins, the cellular localization, or even the conformational change of PTEN should be done in the future.

Previous studies described that PTEN binding stabilizes p53, which in turn results in an elevated p53 abundance [68]. Other researchers indicated that p44/42 MAPK activation is also

related to the PTEN protein phosphatase activity [72]. In this study, a PTEN inhibitor not only reversed EA-caused AKT inactivation but also diminished the p53 upregulation and the dephosphorylation of p44/42 MAPK. These observations also support my hypothesis that EA acts as a PTEN regulator. Then, what are mechanisms on inducing G1 arrest without p53 activity? PTEN and AKT signaling pathways play various roles in Cell cycle control. Besides upregulation of p53, some previous studies showed that PTEN is able to increase p27 protein levels[79]. In addition, inhibition of AKT pathway keeps cyclin D1 from localizing to the nucleus[80]. Moreover, AKT was found to directly phosphorylate p21 and p27, preventing their nuclear translocation[18,19]; namely, inhibition of AKT released the inhibition proteins into the nucleus, where they bind to and inactivate the CDKs. All would be possible mechanisms of inducing G1 arrest without p53 activity. However, I still need some more direct observations on how the relationship between PTEN and p53 changes in EA treatments. Last, further investigation of EA effects on p53-deficient cancer cell line is necessary to reveal the exact mechanism.

But yet, without doubt, this is the first evidence that EA is related to the regulation of PTEN activity, and its reversible property further underscores its potential as a convenient tool to study PTEN functions in living cells.

Feedback activation of AKT during treatments of patients with PI3K inhibitors is often an annoying problem in cancer therapy as well as biological experiments. EA inhibits AKT activation in a different way from the PI3K inhibitors, providing a novel tool to achieve prolonged AKT inactivation. Moreover, EA mitigated the PI3K inhibitor-caused later enhancement of AKT phosphorylation, and therefore, EA may provide a way investigating the feedback activation pathway. Therefore, as an alternative to PI3K inhibitors, EA may be useful for studying AKT-related signaling pathways.

It has been suggested that in some cancer cell lines, cisplatin treatment activates the AKT signaling pathway, which, in turn, prevents the cell death[76]. I demonstrated that EA ultimately

caused the attenuation of AKT signaling. Indeed, I showed that a combination of EA and cisplatin synergistically induced B16F10 cell deaths. Interestingly, previous research has shown that EA could protect hepatic cells and testicular cells from apoptosis in cisplatin treatments [47,81,82], seemingly contrary to my observations with B16F10 cells. However, these reports studied normal cells, and therefore further highlight the potential usefulness of the combination of EA and cisplatin in cancer therapy, since the combination appears to be beneficial to normal cells but toxic to cancer cells. The combination treatment of EA and cisplatin is expected to induce cancer cell death more effectively. It goes without saying, however, that much work, including *in vivo* experiments, will be needed to study for tumor specificity, unexpected side effects, or other possible limitations to the combined treatment strategy before the application of clinical trial.

5. References

1 Hanahan, D. & Weinberg, R. A. Hallmarks of cancer: the next generation. *Cell* **144**, 646-674, doi:10.1016/j.cell.2011.02.013 (2011).

2 Luo, J., Solimini, N. L. & Elledge, S. J. Principles of cancer therapy: oncogene and non-oncogene addiction. *Cell* **136**, 823-837, doi:10.1016/j.cell.2009.02.024 (2009).

3 Hartwell, L. H. & Kastan, M. B. Cell cycle control and cancer. *Science* **266**, 1821-1828 (1994).

4 Schafer, K. A. The cell cycle: a review. *Vet Pathol* **35**, 461-478, doi:10.1177/030098589803500601 (1998).

5 Grana, X. & Reddy, E. P. Cell cycle control in mammalian cells: role of cyclins, cyclin dependent kinases (CDKs), growth suppressor genes and cyclin-dependent kinase inhibitors (CKIs). *Oncogene* **11**, 211-219 (1995).

6 Pavletich, N. P. Mechanisms of cyclin-dependent kinase regulation: structures of Cdks, their cyclin activators, and Cip and INK4 inhibitors. *J Mol Biol* **287**, 821-828, doi:10.1006/jmbi.1999.2640 (1999).

7 Besson, A., Dowdy, S. F. & Roberts, J. M. CDK inhibitors: cell cycle regulators and beyond. *Dev Cell* **14**, 159-169, doi:10.1016/j.devcel.2008.01.013 (2008).

8 Fresno Vara, J. A. *et al.* PI3K/Akt signalling pathway and cancer. *Cancer Treat Rev* **30**, 193-204, doi:10.1016/j.ctrv.2003.07.007 (2004).

9 Roberts, P. J. & Der, C. J. Targeting the Raf-MEK-ERK mitogen-activated protein kinase cascade for the treatment of cancer. *Oncogene* **26**, 3291-3310, doi:10.1038/sj.onc.1210422 (2007).

10 McCubrey, J. A. *et al.* Roles of the RAF/MEK/ERK and PI3K/PTEN/AKT pathways in malignant transformation and drug resistance. *Adv Enzyme Regul* **46**, 249-279, doi:10.1016/j.advenzreg.2006.01.004 (2006).

11 Muller, P. A. & Vousden, K. H. p53 mutations in cancer. *Nat Cell Biol* **15**, 2-8, doi:10.1038/ncb2641 (2013).

12 Olivier, M., Hollstein, M. & Hainaut, P. TP53 mutations in human cancers: origins, consequences, and clinical use. *Cold Spring Harb Perspect Biol* **2**, a001008, doi:10.1101/cshperspect.a001008 (2010).

13 Hollander, M. C., Blumenthal, G. M. & Dennis, P. A. PTEN loss in the continuum of common cancers, rare syndromes and mouse models. *Nat Rev Cancer* **11**, 289-301, doi:10.1038/nrc3037 (2011).

14 Song, M. S., Salmena, L. & Pandolfi, P. P. The functions and regulation of the PTEN tumour suppressor. *Nat Rev Mol Cell Biol* **13**, 283-296, doi:10.1038/nrm3330 (2012).

15 Walker, J. L. & Assoian, R. K. Integrin-dependent signal transduction regulating cyclin D1 expression and G1 phase cell cycle progression. *Cancer Metastasis Rev* **24**, 383-393, doi:10.1007/s10555-005-5130-7 (2005).

16 Moreno-Layseca, P. & Streuli, C. H. Signalling pathways linking integrins with cell cycle progression. *Matrix Biol* **34**, 144-153, doi:10.1016/j.matbio.2013.10.011 (2014).

17 Musgrove, E. A., Caldon, C. E., Barraclough, J., Stone, A. & Sutherland, R. L. Cyclin D as a therapeutic target in cancer. *Nat Rev Cancer* **11**, 558-572, doi:10.1038/nrc3090 (2011).

18 Liang, J. *et al.* PKB/Akt phosphorylates p27, impairs nuclear import of p27 and opposes p27-mediated G1 arrest. *Nat Med* **8**, 1153-1160, doi:10.1038/nm761 (2002).

19 Abbas, T. & Dutta, A. p21 in cancer: intricate networks and multiple activities. *Nat Rev Cancer* **9**, 400-414, doi:10.1038/nrc2657 (2009).

20 Ogawara, Y. *et al.* Akt enhances Mdm2-mediated ubiquitination and degradation of p53. *J Biol Chem* **277**, 21843-21850, doi:10.1074/jbc.M109745200 (2002).

21 Holsberger, D. R. & Cooke, P. S. Understanding the role of thyroid hormone in Sertoli cell development: a mechanistic hypothesis. *Cell Tissue Res* **322**, 133-140, doi:10.1007/s00441-005-1082-z (2005).

22 Bertoli, C., Skotheim, J. M. & de Bruin, R. A. Control of cell cycle transcription during G1 and S phases. *Nat Rev Mol Cell Biol* **14**, 518-528, doi:10.1038/nrm3629 (2013).

23 Carnero, A., Blanco-Aparicio, C., Renner, O., Link, W. & Leal, J. F. The PTEN/PI3K/AKT signalling pathway in cancer, therapeutic implications. *Curr Cancer Drug Targets* **8**, 187-198 (2008).

24 Fruman, D. A. *et al.* The PI3K Pathway in Human Disease. *Cell* **170**, 605-635, doi:10.1016/j.cell.2017.07.029 (2017).

25 Vanhaesebroeck, B. & Alessi, D. R. The PI3K-PDK1 connection: more than just a road to PKB. *Biochem J* **346 Pt 3**, 561-576 (2000).

26 Beurel, E., Grieco, S. F. & Jope, R. S. Glycogen synthase kinase-3 (GSK3): regulation, actions, and diseases. *Pharmacol Ther* **148**, 114-131, doi:10.1016/j.pharmthera.2014.11.016 (2015).

27 Polivka, J., Jr. & Janku, F. Molecular targets for cancer therapy in the PI3K/AKT/mTOR pathway. *Pharmacol Ther* **142**, 164-175, doi:10.1016/j.pharmthera.2013.12.004 (2014).

28 Thorpe, L. M., Yuzugullu, H. & Zhao, J. J. PI3K in cancer: divergent roles of isoforms, modes of activation and therapeutic targeting. *Nat Rev Cancer* **15**, 7-24, doi:10.1038/nrc3860 (2015).

29 Wong, K. K., Engelman, J. A. & Cantley, L. C. Targeting the PI3K signaling pathway in cancer. *Curr Opin Genet Dev* **20**, 87-90, doi:10.1016/j.gde.2009.11.002 (2010).

30 Austin, M. T., Xing Y Fau - Hayes-Jordan, A. A., Hayes-Jordan Aa Fau - Lally, K. P., Lally Kp Fau - Cormier, J. N. & Cormier, J. N. Melanoma incidence rises for children and adolescents: an epidemiologic review of pediatric melanoma in the United States.

31 Markovic, S. N. Malignant melanoma in the 21st century, part 1: epidemiology, risk factors, screening, prevention, and diagnosis.

32 Balch, C. M. *et al.* Final version of 2009 AJCC melanoma staging and classification. *J Clin Oncol* **27**, 6199-6206, doi:10.1200/jco.2009.23.4799 (2009).

33 Chapman, P. B. *et al.* Phase III multicenter randomized trial of the Dartmouth regimen versus dacarbazine in patients with metastatic melanoma. *J Clin Oncol* **17**, 2745-2751, doi:10.1200/jco.1999.17.9.2745 (1999).

34 Sasse, A. D., Sasse, E. C., Clark, L. G., Ulloa, L. & Clark, O. A. Chemoimmunotherapy versus chemotherapy for metastatic malignant melanoma. *Cochrane Database Syst Rev*, Cd005413, doi:10.1002/14651858.CD005413.pub2 (2007).

35 Jemal, A. *et al.* Recent trends in cutaneous melanoma incidence and death rates in the United States, 1992-2006. *J Am Acad Dermatol* **65**, S17-25.e11-13, doi:10.1016/j.jaad.2011.04.032 (2011).

36 Malas, S., Harrasser, M., Lacy, K. E. & Karagiannis, S. N. Antibody therapies for melanoma: new and emerging opportunities to activate immunity (Review). *Oncol Rep* **32**, 875-886, doi:10.3892/or.2014.3275 (2014).

37 Hendriks, D., Choi, G., de Bruyn, M., Wiersma, V. R. & Bremer, E. Antibody-Based Cancer Therapy: Successful Agents and Novel Approaches. *Int Rev Cell Mol Biol* **331**, 289-383, doi:10.1016/bs.ircmb.2016.10.002 (2017).

38 Sasaoka, N. *et al.* Long-term oral administration of hop flower extracts mitigates Alzheimer phenotypes in mice. *PLoS One* **9**, e87185, doi:10.1371/journal.pone.0087185 (2014).

39 Lee, N. H. *et al.* Anti-asthmatic effect of Sanguisorba officinalis L. and potential role of heme oxygenase-1 in an ovalbumin-induced murine asthma model. *Int J Mol Med* **26**, 201-208 (2010).

40 Zhang, S. *et al.* Isolation and identification of the phenolic compounds from the roots of Sanguisorba officinalis L. and their antioxidant activities. *Molecules (Basel, Switzerland)* **17**, 13917-13922, doi:10.3390/molecules171213917 (2012).

41 Jang, E., Inn, K. S., Jang, Y. P., Lee, K. T. & Lee, J. H. Phytotherapeutic Activities of Sanguisorba officinalis and its Chemical Constituents: A Review. *Am J Chin Med* **46**, 299-318, doi:10.1142/s0192415x18500155 (2018).

42 Zhu, X. *et al.* Ziyuglycoside II inhibits the growth of human breast carcinoma MDA-MB-435 cells via cell cycle arrest and induction of apoptosis through the mitochondria dependent pathway. *Int J Mol Sci* **14**, 18041-18055, doi:10.3390/ijms140918041 (2013).

43 Zhu, A. K. *et al.* Ziyuglycoside II-induced apoptosis in human gastric carcinoma BGC-823 cells by regulating Bax/Bcl-2 expression and activating caspase-3 pathway. *Braz J Med Biol Res* **46**, 670-675, doi:10.1590/1414-431x20133050 (2013).

44 Goriparti, S., Harish, M. N. & Sampath, S. Ellagic acid--a novel organic electrode material for high capacity lithium ion batteries. *Chem Commun (Camb)* **49**, 7234-7236, doi:10.1039/c3cc43194k (2013).

45 Tang, Y. Y. *et al.* Polyphenols and Alkaloids in Byproducts of Longan Fruits (Dimocarpus Longan Lour.) and Their Bioactivities. *Molecules* **24**, doi:10.3390/molecules24061186 (2019).

46 Falcao, T. R. *et al.* Crude extract from Libidibia ferrea (Mart. ex. Tul.) L.P. Queiroz leaves decreased intra articular inflammation induced by zymosan in rats. *BMC Complement Altern Med* **19**, 47, doi:10.1186/s12906-019-2454-3 (2019).

47 Garcia-Nino, W. R. & Zazueta, C. Ellagic acid: Pharmacological activities and molecular mechanisms involved in liver protection. *Pharmacological research* **97**, 84-103, doi:10.1016/j.phrs.2015.04.008 (2015).

48 Shimogaki, H., Tanaka, Y., Tamai, H. & Masuda, M. In vitro and in vivo evaluation of ellagic acid on melanogenesis inhibition. *Int J Cosmet Sci* **22**, 291-303, doi:10.1046/j.1467-2494.2000.00023.x (2000).

49 Kowshik, J. *et al.* Ellagic acid inhibits VEGF/VEGFR2, PI3K/Akt and MAPK signaling cascades in the hamster cheek pouch carcinogenesis model. *Anticancer Agents Med Chem* **14**, 1249-1260 (2014).

50 Chen, H. S., Bai, M. H., Zhang, T., Li, G. D. & Liu, M. Ellagic acid induces cell cycle arrest and apoptosis through TGF-beta/Smad3 signaling pathway in human breast cancer MCF-7 cells. *Int J Oncol* **46**, 1730-1738, doi:10.3892/ijo.2015.2870 (2015).

51 Cheng, H. *et al.* Ellagic acid inhibits the proliferation of human pancreatic carcinoma PANC-1 cells in vitro and in vivo. *Oncotarget* **8**, 12301-12310, doi:10.18632/oncotarget.14811 (2017).

52 Luo, C. & Shen, J. Research progress in advanced melanoma. *Cancer Lett* **397**, 120-126, doi:10.1016/j.canlet.2017.03.037 (2017).

53 Zebary, A. *et al.* KIT, NRAS, BRAF and PTEN mutations in a sample of Swedish patients with acral lentiginous melanoma. *J Dermatol Sci* **72**, 284-289, doi:10.1016/j.jdermsci.2013.07.013 (2013).

54 Jakob, J. A. *et al.* NRAS mutation status is an independent prognostic factor in metastatic melanoma. *Cancer* **118**, 4014-4023, doi:10.1002/cncr.26724 (2012).

55 Umesalma, S., Nagendraprabhu, P. & Sudhandiran, G. Ellagic acid inhibits proliferation and induced apoptosis via the Akt signaling pathway in HCT-15 colon adenocarcinoma cells. *Mol Cell Biochem* **399**, 303-313, doi:10.1007/s11010-014-2257-2 (2015).

56 Li, T. M. *et al.* Ellagic acid induced p53/p21 expression, G1 arrest and apoptosis in human bladder cancer T24 cells. *Anticancer Res* **25**, 971-979 (2005).

57 Dufner, A. & Thomas, G. Ribosomal S6 kinase signaling and the control of translation. *Exp Cell Res* **253**, 100-109, doi:10.1006/excr.1999.4683 (1999).

58 Scheid, M. P., Marignani, P. A. & Woodgett, J. R. Multiple phosphoinositide 3-kinase-dependent steps in activation of protein kinase B. *Mol Cell Biol* **22**, 6247-6260 (2002).

59 Murphy, L. O. & Blenis, J. MAPK signal specificity: the right place at the right time. *Trends Biochem Sci* **31**, 268-275, doi:10.1016/j.tibs.2006.03.009 (2006).

60 Olsen, B. B., Svenstrup, T. H. & Guerra, B. Downregulation of protein kinase CK2 induces autophagic cell death through modulation of the mTOR and MAPK signaling pathways in human glioblastoma cells. *Int J Oncol* **41**, 1967-1976, doi:10.3892/ijo.2012.1635 (2012).

61 Ryu, S. Y. & Kim, S. Evaluation of CK2 inhibitor (E)-3-(2,3,4,5-tetrabromophenyl)acrylic acid (TBCA) in regulation of platelet function. *Eur J Pharmacol* **720**, 391-400, doi:10.1016/j.ejphar.2013.09.064 (2013).

62 So, K. S. *et al.* AKT/mTOR down-regulation by CX-4945, a CK2 inhibitor, promotes apoptosis in chemorefractory non-small cell lung cancer cells. *Anticancer Res* **35**, 1537-1542 (2015).

63 Dixit, D., Sharma, V., Ghosh, S., Mehta, V. S. & Sen, E. Inhibition of Casein kinase-2 induces p53-dependent cell cycle arrest and sensitizes glioblastoma cells to tumor necrosis factor (TNFalpha)-induced apoptosis through SIRT1 inhibition. *Cell Death Dis* **3**, e271, doi:10.1038/cddis.2012.10 (2012).

64 Cozza, G. *et al.* Identification of ellagic acid as potent inhibitor of protein kinase CK2: a successful example of a virtual screening application. *J Med Chem* **49**, 2363-2366, doi:10.1021/jm060112m (2006).

65 Komarov, P. G. *et al.* A chemical inhibitor of p53 that protects mice from the side effects of cancer therapy. *Science* **285**, 1733-1737 (1999).

66 Rosivatz, E. *et al.* A small molecule inhibitor for phosphatase and tensin homologue deleted on chromosome 10 (PTEN). *ACS Chem Biol* **1**, 780-790, doi:10.1021/cb600352f (2006).

67 Vlahos, C. J., Matter, W. F., Hui, K. Y. & Brown, R. F. A specific inhibitor of phosphatidylinositol 3-kinase, 2-(4-morpholinyl)-8-phenyl-4H-1-benzopyran-4-one (LY294002). *J Biol Chem* **269**, 5241-5248 (1994).

68 Freeman, D. J. *et al.* PTEN tumor suppressor regulates p53 protein levels and activity through phosphatase-dependent and -independent mechanisms. *Cancer Cell* **3**, 117-130 (2003).

69 Myers, M. P. *et al.* P-TEN, the tumor suppressor from human chromosome 10q23, is a dual-specificity phosphatase. *Proc Natl Acad Sci U S A* **94**, 9052-9057 (1997).

70 Tamura, M. *et al.* PTEN interactions with focal adhesion kinase and suppression of the extracellular matrix-dependent phosphatidylinositol 3-kinase/Akt cell survival pathway. *J Biol Chem* **274**, 20693-20703 (1999).

71 Sonoda, Y., Watanabe, S., Matsumoto, Y., Aizu-Yokota, E. & Kasahara, T. FAK is the upstream signal protein of the phosphatidylinositol 3-kinase-Akt survival pathway in hydrogen peroxide-induced apoptosis of a human glioblastoma cell line. *J Biol Chem* **274**, 10566-10570 (1999).

72 Gu, J. *et al.* Shc and FAK differentially regulate cell motility and directionality modulated by PTEN. *J Cell Biol* **146**, 389-403 (1999).

73 Le, X. *et al.* Systematic Functional Characterization of Resistance to PI3K Inhibition in Breast Cancer. *Cancer Discov* **6**, 1134-1147, doi:10.1158/2159-8290.cd-16-0305 (2016).

74 Fruman, D. A. & Rommel, C. PI3K and cancer: lessons, challenges and opportunities. *Nat Rev Drug Discov* **13**, 140-156, doi:10.1038/nrd4204 (2014).

75 Dasari, S. & Tchounwou, P. B. Cisplatin in cancer therapy: molecular mechanisms of action. *Eur J Pharmacol* **740**, 364-378, doi:10.1016/j.ejphar.2014.07.025 (2014).

76 Galluzzi, L. *et al.* Molecular mechanisms of cisplatin resistance. *Oncogene* **31**, 1869-1883, doi:10.1038/onc.2011.384 (2012).

77 Gao, X., Wu, J., Zou, W. & Dai, Y. Two ellagic acids isolated from roots of Sanguisorba officinalis L. promote hematopoietic progenitor cell proliferation and megakaryocyte differentiation. *Molecules (Basel, Switzerland)* **19**, 5448-5458, doi:10.3390/molecules19045448 (2014).

78 Wang, Z. *et al.* Effect of Sanguisorba officinalis L on breast cancer growth and angiogenesis. *Expert opinion on therapeutic targets* **16 Suppl 1**, S79-89, doi:10.1517/14728222.2011.642371 (2012).

79 Mamillapalli, R. *et al.* PTEN regulates the ubiquitin-dependent degradation of the CDK inhibitor p27(KIP1) through the ubiquitin E3 ligase SCF(SKP2). *Curr Biol* **11**, 263-267, doi:10.1016/s0960-9822(01)00065-3 (2001).

80 Radu, A., Neubauer, V., Akagi, T., Hanafusa, H. & Georgescu, M. M. PTEN induces cell cycle arrest by decreasing the level and nuclear localization of cyclin D1. *Mol Cell Biol* **23**, 6139-6149, doi:10.1128/mcb.23.17.6139-6149.2003 (2003).

81 Al-Kharusi, N. *et al.* Ellagic acid protects against cisplatin-induced nephrotoxicity in rats: a dose-dependent study. *European review for medical and pharmacological sciences* **17**, 299-310 (2013).

82 Turk, G., Ceribasi, A. O., Sahna, E. & Atessahin, A. Lycopene and ellagic acid prevent testicular apoptosis induced by cisplatin. *Phytomedicine : international journal of phytotherapy and phytopharmacology* **18**, 356-361, doi:10.1016/j.phymed.2010.07.008 (2011).

Acknowledgments

First, I would like to thank Professor Akira Kakizuka for providing me the opportunity to do research in the lab in Department of Functional Biology, Division of Systemic Life Science, Kyoto University. I am also grateful to T. Shudo, a chemist in our lab and Doctor Chihiro Zukano, lecturer in Graduate School of Pharmaceutical Sciences, Kyoto University, for helping me with the purification process and performing the structural identification of the purified chemical. I really appreciate Yuma Sugiyama, my research mentor, who taught me a lot with the operation of experiments including the purification processes, cell culture, protein expression analysis, and proposed many ideas in this research. And I also learned a lot from him about data analyzing and how to present the results that are important skills in science study. I am thankful to Si Jia Ying, a master student who studied in Kakizuka lab, for finding that *Sanguisorba officinalis* induced G1 arrest in B16F10 cells. I really thank a lot to Professors James A. Hejna and Kunio Takeyasu (Kyoto University) for critical reading of the manuscript. Last, I'd like to thank my family for supporting me studying in Kyoto University.

This thesis is based on material contained in the following scholarly paper:

Yi Hsun Tan, Toshiyuki Shudo, Tomoki Yoshida, Yuma Sugiyama, Jia Ying Si, Chihiro Tsukano, Yoshiji Takemoto, Akira Kakizuka.

Ellagic acid, extracted from Sanguisorba officinalis, induces G1 arrest by modulating PTEN activity in B16F10 melanoma cells.

Genes to Cells, in press, 2019. DOI:10.1111/gtc.12719